

1
2 ***XAP5 CIRCADIAN TIMEKEEPER* regulates RNA splicing and the**
3 **circadian clock by genetically separable pathways**
4
5

6 **Authors:**

7 Hongtao Zhang (张弘韬)¹, Roderick W. Kumimoto¹, Shajahan Anver^{1,2}, Stacey L. Harmer^{1*}
8

9 **Author affiliations:**

10 ¹Department of Plant Biology, College of Biological Sciences, University of California, Davis,
11 CA 95616, USA

12 ²Department of Genetics, Evolution and Environment, University College London, London, UK
13

14 ***Corresponding author:**

15 slharmer@ucdavis.edu
16

17 **Running title:**

18 Separable roles for *XCT* in splicing and the clock
19
20
21
22
23

24 **Author Contributions**
25

26 HZ, RWK and SLH designed the research; HZ, RWK, and SA performed the research; HZ,
27 RWK, and SLH analyzed data; HZ and SLH wrote the paper.
28
29

30 The author responsible for distribution of materials integral to the findings presented in this
31 article in accordance with the policy described in the Instructions for Authors
32 (<https://academic.oup.com/plphys/pages/General-Instructions>) is Stacey L. Harmer.
33

34 **Abstract**

35 The circadian oscillator allows organisms to synchronize their cellular and physiological
36 activities with diurnal environmental changes. In plants, the circadian clock is primarily
37 composed of multiple transcriptional-translational feedback loops. Regulators of post-
38 transcriptional events, such as pre-mRNA splicing factors, are also involved in controlling the
39 pace of the clock. However, in most cases the underlying mechanisms remain unclear. We have
40 previously identified *XAP5 CIRCADIAN TIMEKEEPER (XCT)* as an *Arabidopsis thaliana*
41 circadian clock regulator with uncharacterized molecular functions. Here, we report that *XCT*
42 physically interacts with components of the spliceosome, including members of the Nineteen
43 Complex (NTC). PacBio Iso-Seq data show that *xct* mutants have transcriptome-wide pre-
44 mRNA splicing defects, predominantly aberrant 3' splice site selection. Expression of a genomic
45 copy of *XCT* fully rescues those splicing defects, demonstrating that functional *XCT* is important
46 for splicing. Dawn-expressed genes are significantly enriched among those aberrantly spliced in
47 *xct* mutants, suggesting that the splicing activity of *XCT* may be circadian regulated. Furthermore,
48 we show that loss-of-function mutations in *PRP19A* or *PRP19B*, two homologous core NTC
49 components, suppress the short circadian period phenotype of *xct-2*. However, we do not see
50 rescue of the splicing defects of core clock genes in *prp19 xct* mutants. Therefore, our results
51 suggest that *XCT* may regulate splicing and the clock function through genetically separable
52 pathways.
53

54 **Introduction**

55 Most eukaryotes have evolved an endogenous timekeeper known as the circadian clock, which
56 allows them to anticipate the daily fluctuating environmental conditions caused by the earth's
57 rotation (Harmer, 2009). Although the central oscillators of circadian clocks in diverse
58 eukaryotes lack conserved individual components, they share similar general architectures
59 (Nohales and Kay, 2016). In plants, the approximately 24-h periodicity of the clock is

60 maintained by a complex gene regulatory network consisting primarily of repressors and
61 activators of transcription. Those regulators, often referred to as core circadian clock genes,
62 regulate each other's expression and the expression of thousands of output genes (Creux and
63 Harmer, 2019).

64
65 Additionally, post-transcriptional and post-translational mechanisms such as alternative splicing
66 of precursor messenger RNAs (pre-mRNAs) provide critical regulation of clock function. It has
67 been suggested that changes in splicing of core circadian clock genes are important for
68 Arabidopsis in response to environmental stresses (James et al., 2012; Kwon et al., 2014). For
69 example, cold temperatures significantly suppress production of a splice variant of *CIRCADIAN*
70 *CLOCK-ASSOCIATED1* (*CCA1*) in which intron four is retained. This incompletely spliced
71 isoform encodes a truncated protein which competitively inhibits the function of fully spliced
72 *CCA1* (Seo et al., 2012). However, in most cases the effects of alternative splicing of pre-
73 mRNAs on circadian clock function remain unclear.

74
75 In contrast, the mechanisms underlying pre-mRNA splicing are increasingly well understood
76 (Wilkinson et al., 2020). There are two catalytic transesterification steps, which sequentially
77 remove first the 5' and then the 3' splice sites (5'SS and 3'SS) of introns from their adjacent
78 exons (Shi, 2017). This process is carried out by five small nuclear ribonucleoproteins (snRNPs)
79 and hundreds of non-snRNP splicing factor proteins which assemble on a pre-mRNA to form the
80 spliceosome complex (Wilkinson et al., 2020). One of these spliceosome complex components is
81 the Nineteen Complex (NTC, also known as PRP19 complex), named after PRECURSOR RNA
82 PROCESSING 19 (PRP19), a U-box E3 ubiquitin ligase that forms the core of the NTC
83 (Hatakeyama et al., 2001; Koncz et al., 2012). The NTC is associated with the spliceosome
84 during the two transesterification steps and helps facilitate conformational rearrangements and
85 promote splicing fidelity (Fig. 1; Hogg et al., 2010). The NTC is highly conserved across
86 eukaryotes. In Arabidopsis, multiple orthologs of yeast NTC proteins including two PRP19
87 homologs (PRP19A/MAC3A and PRP19B/MAC3B) have been shown to physically interact
88 with the spliceosome (Monaghan et al., 2009; Deng et al., 2016). Plants mutant for *prp19a*
89 *prp19b* or homologs of other NTC-associated proteins such as *pleiotropic regulatory locus1*

90 (*prl1*) and *snw/ski-interacting protein (skip)* have genome-wide intron retention defects (Jia et al.,
91 2017; Wang et al., 2012; Li et al., 2019). These data indicate that NTC components act as
92 evolutionarily conserved splicing factors in Arabidopsis.

93
94 Mutation of splicing factors can lead to disruption of circadian clock function (Shakhmantsir and
95 Sehgal, 2019). For example, loss-of-function alleles of NTC components, including *PRP19*,
96 *PRL1* and *SKIP*, cause lengthening of circadian period (Wang et al., 2012; Feke et al., 2019; Li
97 et al., 2019). Aberrantly spliced mRNA variants of core circadian clock genes have been
98 detected in these splicing factor mutants (Sanchez et al., 2010; Wang et al., 2012; Jones et al.,
99 2012; Schlaen et al., 2015; Marshall et al., 2016; Li et al., 2019; Feke et al., 2019), suggesting
100 that changes in the pace of the clock might be caused by aberrant splicing of core clock genes. In
101 some cases, epistasis analysis suggests that this may be true (Marshall et al., 2016; Schlaen et al.,
102 2015). However, in other cases, genetic analysis has either not been performed or has revealed
103 additive interactions between the splicing factor and clock gene mutants. In addition, the levels
104 of mis-spliced mRNA variants of clock genes are usually only a small fraction of total transcripts
105 (Jones et al., 2012; Perez-Santángelo et al., 2014; Feke et al., 2019; Sanchez et al., 2010; Wang
106 et al., 2012). Thus, it is unclear whether splicing factors affect clock function solely by
107 controlling the splicing of core clock genes.

108
109 RNA splicing factors often function in multiple biological pathways: plants deficient for
110 components of the NTC have defects in immunity, microRNA biogenesis, DNA damage
111 response and transcriptional elongation (Koncz et al., 2012; Monaghan et al., 2009; Zhang et al.,
112 2013; Jia et al., 2017). Some splicing factors are known to carry out roles in nuclear processes
113 biochemically separable from their roles in splicing. In addition to its structural role in the
114 spliceosome, PRP19 also senses DNA damage and promotes DNA repair via its ubiquitin ligase
115 activity (Maréchal et al., 2014). Additionally, SKIP acts in two distinct complexes to regulate
116 splicing and the transcription of genes involved in flowering time control (Li et al., 2019).
117 Nonetheless, whether splicing factors might control circadian clock function via splicing-
118 independent activities has not been investigated.

119

120 We previously identified *XAP5 CIRCADIAN TIMEKEEPER (XCT)* as a novel regulator of the
121 Arabidopsis circadian clock (Martin-Tryon and Harmer, 2008). Like NTC components, *XCT* is
122 also well-conserved across eukaryotes. Homologs of *XCT* (also known as *XAP5* proteins) share
123 a highly conserved C-terminal protein domain and are nuclear-localized (Martin-Tryon and
124 Harmer, 2008; Anver et al., 2014; Li et al., 2018; Lee et al., 2020). Previously, we found that
125 transgenic expression of Arabidopsis *XCT* fully rescued the slow-growth phenotype of fission
126 yeast mutant for *xap5* (Anver et al., 2014). Taken together, these data suggest that *XCT*
127 homologs might share similar molecular and cellular functions across kingdoms.

128
129 It has been reported that *FAM50A*, one of the two *XCT* orthologs in humans, physically
130 associates with the spliceosomal C complex and its mutants have defects in RNA splicing
131 (Bessonov et al., 2008; Lee et al., 2020). Similarly, a recent study in Arabidopsis also reported
132 the association of *XCT* with the spliceosome (Liu et al., 2022), implying that *XAP5* proteins may
133 be evolutionarily conserved splicing factors. However, evidence suggests that *XAP5* proteins
134 may also participate in fundamental biological processes other than splicing. Fission yeast and
135 *Chlamydomonas* *XAP5* proteins associate with chromatin and directly regulate transcription
136 (Anver et al., 2014; Li et al., 2018). In addition to its role in the clock, Arabidopsis *XCT* has been
137 implicated in diverse processes including small RNA production, immune signaling, and DNA
138 damage responses (Fang et al., 2015; Xu et al., 2017; Kumimoto et al., 2021). Notably, NTC
139 components have also been reported to function in all these pathways (Jia et al., 2017; Maréchal
140 et al., 2014; Chanarat and Sträßer, 2013). Although pleiotropic defects are seen in *xct* mutants,
141 interconnections between these phenotypes and the molecular function of *XCT* have not been
142 extensively studied.

143
144 In the current work, we report that *XCT* physically interacts with NTC and other spliceosome-
145 associated proteins in Arabidopsis. We use long-read RNA sequencing to reveal that *XCT*
146 controls the fidelity of 3' splice site selection for hundreds of pre-mRNA splicing events,
147 probably by rejecting downstream suboptimal 3' splice sites. Intriguingly, circadian-regulated
148 genes that are aberrantly spliced in *xct* mutants are significantly enriched for peak expression at
149 subjective dawn. This implies that the splicing-related activity of *XCT* may be circadian

150 regulated. We also demonstrate that *PRP19A* and *PRP19B* display epistatic genetic interactions
151 with *XCT* in control of the circadian clock period length but not of the splicing of core clock
152 genes. This is consistent with our finding that although *xct-2* causes more severe splicing defects
153 than *xct-1*, *xct-1* mutants have a stronger circadian phenotype. Collectively, our results suggest
154 that *XCT* works close to *NTC* and may regulate pre-mRNA splicing and the circadian clock
155 function via distinct pathways.

156

157 **Results**

158 ***XCT* physically interacts with the Nineteen Complex and other spliceosome-associated** 159 **proteins**

160

161 To uncover the molecular functions of *XCT*, we carried out mass spectrometry (MS)
162 experiments to identify its possible interactors. We expressed epitope-tagged *XCT* protein under
163 the control of the native *XCT* promoter in *xct-2* mutant background (*xct-2 XCT*). This transgene
164 largely rescued the morphological and circadian clock defects of *xct-2* (Supplemental Fig. S1).
165 Next, we affinity purified tagged *XCT* from plant extracts and analyzed co-purifying proteins via
166 MS. In total, 26 proteins were significantly enriched in the *XCT* immunoprecipitation compared
167 to control immunoprecipitations (Welch's two sample *t*-test, $P < 0.05$; Supplemental Dataset S1).
168 Among those *XCT*-associated proteins, 15 (57.7%) were annotated as mRNA splicing-related,
169 including 11 core *NTC* or *NTC*-associated proteins (Table 1), consistent with the MS and co-
170 immunoprecipitation data from a recent report (Liu et al., 2022). Notably, studies in human and
171 yeast have revealed that *NTC* is physically associated with the spliceosomal complex throughout
172 the two catalytic transesterification steps (Fig. 1; Hogg et al., 2010). Taken together, those results
173 imply that *XCT* may act close to *NTC* and function in the catalytic steps during pre-mRNA
174 splicing. Interestingly, we also observed 8 (30.8%) chloroplast proteins enriched in the *XCT*
175 immunoprecipitation (Supplemental Dataset S1), which may be related to the delayed leaf
176 greening phenotypes observed in *xct-2* mutant plants (Martin-Tryon and Harmer, 2008).

177

178 ***XCT* is required for the fidelity of 3' splice site selection during pre-mRNA splicing**

179

180 To investigate a possible role for *XCT* in RNA splicing, we performed PacBio Isoform
181 Sequencing (Iso-Seq) on wild-type Col-0, reduction-of-function allele *xct-1*, null allele *xct-2*, and
182 the complemented line *xct-2 XCT*. Additionally, we also sequenced *prll-2*, which contains a T-
183 DNA insertion mutation in *PRL1*, an NTC member that has been demonstrated to control
184 genome-wide splicing efficiency (Jia et al., 2017). Since both transcript levels and RNA splicing
185 of a large proportion of the Arabidopsis transcriptome are circadian regulated (Romanowski et
186 al., 2020; Yang et al., 2020), the time of day at which plants are harvested has significant effects
187 on gene expression and splicing analysis (Hsu and Harmer, 2012). Therefore, we grew plants in
188 constant environmental conditions for ten days to desynchronize clocks of individual plants. To
189 further minimize any differences in subjective time of day between wild-type plants, the long-
190 circadian-period *prll-2*, and the short-period *xct* mutants (Supplemental Fig. S2), we pooled
191 seedlings harvested at 2-hour intervals across a twenty-four hour period (Fig. 2A). For each
192 genotype, we sequenced three biological replicates and acquired an average of 784,832 full-
193 length transcript reads per genotype per replicate (Supplemental Dataset S2). With no alignment
194 needed, those reads were directly mapped to the TAIR 10 Arabidopsis reference genome and
195 then subjected to differential splicing analysis using the JunctionSeq R package (Hartley and
196 Mullikin, 2016).

197
198 Previous studies have demonstrated that intron retention is the most prevalent type of alternative
199 splicing event in Arabidopsis (Wang and Brendel, 2006; Filichkin et al., 2010). Indeed, plants
200 mutant for multiple NTC components have been reported to have global intron retention defects
201 (Jia et al., 2017; Meng et al., 2022). In our analysis of *prll-2*, we found 5,730 out of 44,496
202 detected splicing events were significantly differentially enriched from Col-0 (Supplemental
203 Dataset S3). Notably, 99% of these events were decreases in known junctions (Supplemental Fig.
204 S3), consistent with previous studies suggesting that loss of *PRL1* function mainly causes intron
205 retention without affecting splice site selection (Jia et al., 2017).

206
207 We next examined transcript composition in *xct* mutants. In the null allele *xct-2*, we detected
208 75,073 splicing events, of which 875 were significantly down-regulated and 532 were up-
209 regulated compared with Col-0 (FDR<0.05, Fig. 2B-C). Meanwhile, 209 and 337 splicing events

210 were significantly decreased or increased, respectively, in the partial loss-of-function mutant *xct-*
211 *1*. Comparing mis-regulated splicing between the two *xct* mutant alleles, 196 (93.8%) of the
212 down-regulated and 329 (97.6%) of the up-regulated events were shared. Thus, the two *xct*
213 alleles have similar splicing phenotypes but the severity of the defect is greater in the null allele
214 despite the stronger effect of *xct-1* on circadian period (Supplemental Fig. S1). Next, we
215 analyzed the splicing events in the complemented line *xct-2 XCT*. Only 16 out of 84,965 events
216 were significantly differentially enriched compared with Col-0, indicating that the splicing
217 defects of *xct-2* were almost completely rescued by the restored *XCT* expression. Taken together,
218 these results demonstrate that *XCT* is important for transcriptome-wide pre-mRNA splicing.

219
220 To further characterize the major types of splicing defects caused by loss of *XCT* function, we
221 analyzed the splice sites for the differentially spliced junctions in *xct* mutants. Specifically, we
222 categorized *xct*-induced mis-splicing events into four classes based on whether the 5' and 3'
223 splice sites used were previously annotated (known) or not (novel). As expected, most down-
224 regulated splicing events displayed decreases in usage of junctions with known 5' and 3' splice
225 sites (Fig. 2D). Interestingly, 307 (90.8%) in *xct-1* and 462 (86.5%) in *xct-2* of up-regulated
226 splicing events involved increased usage of junctions with a known 5' splice site but a novel 3'
227 splice site (Fig. 2E). The decreases in abundance of junctions with known splice sites hence
228 reflects both intron retention events and novel 3' splice sites usage. Therefore, our results
229 demonstrate that in addition to controlling the efficient removal of introns, *XCT* is also
230 responsible for the fidelity of 3' splice site selection.

231
232 To investigate how *XCT* contributes to the fidelity of 3' splice site selection, we compared the
233 significantly up- or down-regulated 3' splice sites in *xct* mutants with all detected 3' splice sites
234 in Col-0. Intriguingly, most of the up-regulated novel 3' splice sites in *xct-1* and *xct-2* were
235 located less than 50 nucleotides downstream of the wild-type 3' splice sites (Fig. 3B;
236 Supplemental Fig. S4A). Studies in human and yeast have demonstrated that the sequences
237 preceding a 3' splice site, including the polypyrimidine tract (PPT) and the pyrimidine at the -3
238 position (Fig. 3A), are important for the strength of the 3' splice site (Horowitz, 2012). Therefore,
239 we further examined the 23-mer sequences flanking the 3' splice sites (from -20 to +3 position).

240 We found that the frequency of the canonical AG sequence at the 3' splice sites was not altered
241 in either *xct-1* or *xct-2* (Fig. 3C; Supplemental Fig. S4B-C). However, the average predicted
242 strength of the 875 down-regulated 3' splice sites in *xct-2* was significantly weaker than the
243 average of total detected 3' splice sites in Col-0 (Fig. 3D). Specifically, the percentage of
244 pyrimidine residues at the -3 position was significantly reduced in down-regulated 3' splice sites
245 compared to that found in all detected 3' splice sites (Fisher's exact test, $P < 0.001$, Fig. 3E),
246 suggesting that functional *XCT* is important for the removal of 3' splice sites with a suboptimal
247 sequence at the -3 position. Moreover, the 532 up-regulated 3' splice sites had an even lower 3'
248 splice site score than the down-regulated sites (Fig. 3D). The frequency of pyrimidines both at
249 the -3 position and throughout the PPT region was significantly lower in the up-regulated
250 junctions (Fig. 3E-F), showing that *xct-2* is less able to discriminate between 3' splice sites
251 during splicing. Taken together, our Iso-Seq data demonstrates that *XCT* controls the accuracy of
252 3' splice site selection, possibly by helping to recognize weaker 3' splice sites and reject sub-
253 optimal downstream sites.

254

255 **The splicing defects of core clock genes are generally more severe in *xct-2* than *xct-1***

256

257 Since aberrant splicing of core clock genes may fully or partially contribute to the altered
258 circadian clock period phenotype in splicing factor mutants (Sanchez et al., 2010; Wang et al.,
259 2012; Jones et al., 2012; Schlaen et al., 2015; Marshall et al., 2016; Li et al., 2019; Fekete et al.,
260 2019), we searched for core clock genes with aberrant splicing events in both the short-period
261 *xct-1* and *xct-2* mutants. In total, our Iso-Seq data detected five aberrantly spliced core clock
262 genes, including *LHY*, *LNK2*, *PRR7*, *TOC1* and *TIC* (Fig. 4A). However, we noticed that the
263 ratio of aberrantly-spliced relative to fully-spliced transcripts for several clock genes are
264 significantly higher in *xct-2* than *xct-1*, even though the circadian period defect is more severe in
265 the latter (Supplemental Fig. S5A-D; Supplemental Fig. S1B). We confirmed this finding via
266 semi-qRT-PCR assay (Supplemental Fig. S5E-H). Thus, those results imply that there may be a
267 disconnect between the splicing and circadian clock defects in *xct-1* and *xct-2*.

268

269 **Genes expressed at subjective dawn are enriched among those aberrantly spliced in *xct***
270 **mutants**

271
272 To more broadly explore possible links between the circadian clock and splicing phenotypes in
273 *xct* mutants, we looked for enrichment of circadian clock regulation within genes aberrantly
274 spliced in *xct*. Among the 5,602 previously reported clock-regulated genes (Romanowski et al.,
275 2020) that are detected in our Iso-Seq data, we identified 182 and 402 genes that are mis-spliced
276 in *xct-1* and *xct-2*, respectively (Fig. 4A; Supplemental Dataset S4). However, there is no
277 significant over-representation in either mutant (one-tailed Fisher's exact test, $P = 0.87$ for *xct-1*
278 and 0.99 for *xct-2*), suggesting that *XCT* does not preferentially affect the splicing of clock-
279 regulated genes.

280
281 Previous studies have identified transcripts that are differentially spliced at various times of day
282 (Romanowski et al., 2020; Yang et al., 2020). This suggests that splicing activity may be
283 circadian clock regulated. Therefore, to test whether *XCT* preferentially affects pre-mRNA
284 splicing at certain times of day, we examined the distribution of estimated peak expression times
285 of genes aberrantly spliced in *xct* mutants. We grouped all 5,602 clock-regulated genes into
286 twelve 2-hour intervals based on their estimated peak expression time (Fig. 4B). Genes that are
287 aberrantly spliced in *xct-2* are significantly enriched for peak expression between ZT22 and ZT2
288 compared with the other intervals of the day (Fig. 4C-D, Fisher's exact test, $P < 1e-4$). Similarly,
289 clock-regulated genes that are aberrantly spliced in *xct-1* also showed a dawn-enriched
290 expression pattern (Supplemental Fig. S6). Collectively, those results indicate that *XCT* activity
291 within the spliceosome may be regulated by the circadian clock.

292
293 To further investigate whether *XCT* preferentially affects splicing of transcripts produced at
294 dawn, we monitored the abundance of candidate splice variants via quantitative reverse
295 transcriptase-polymerase chain reaction (qRT-PCR) over a 24-hour light/dark period (LD)
296 followed by 48 hours in constant light (LL). We selected four circadian-clock-regulated genes
297 and one non-clock-regulated gene that are aberrantly spliced in *xct-2* and fully rescued in *xct-2*
298 *XCT* (Fig. 5A-E). Total transcript levels of clock-regulated genes displayed rhythmic abundance

299 with peak *LHY* and *LNK2* expression at dawn and peak *PRR7* and *TOC1* expression late in the
300 afternoon (Supplemental Fig. S7), as expected (Creux and Harmer, 2019). We found
301 significantly advanced phases of expression in *xct-2* but this mutation did not affect the overall
302 abundance of total transcripts for those genes. However, both the peak and average abundance of
303 the aberrantly spliced isoforms were significantly different in *xct-2* compared with Col-0 (Fig.
304 5F-J). This serves as validation of the pooling strategy we used to generate our Iso-Seq libraries,
305 where the daily abundance of transcripts was averaged (Fig. 2A; Fig. 5A-E). Contrary to our
306 expectations, instead of preferentially accumulating at dawn, abundance of all splice variants in
307 *xct-2* was synchronized with total transcript levels (Fig. 5F-I; Supplemental Fig. S7). Likewise,
308 the mis-spliced isoform of the non-clock-regulated gene *SPPA* did not show a significant
309 morning peak (Fig. 5J). Meanwhile, the genomic *XCT* complemented line almost completely
310 rescued the splicing defects across the whole experimental period. Taken together, those results
311 suggest that although morning-expressed genes are preferentially enriched among *XCT* targets,
312 *XCT* is important for the accuracy of pre-mRNA splicing throughout the day under both LD and
313 free-running LL conditions.

314

315 **Reduction of *PRP19* function rescues the circadian clock but not the splicing defects in *xct-*** 316 **2**

317

318 Previous studies revealed that NTC components participate in regulation of circadian clock
319 function in Arabidopsis (Feke et al., 2019; Li et al., 2019). Here we examined circadian period in
320 mutants for several NTC components. We found that mutation in either of the two Arabidopsis
321 *PRP19* homologs, *PRP19A* (*MAC3A*) or *PRP19B* (*MAC3B*), only caused minor lengthening of
322 circadian period. In contrast, the *prp19a-1 prp19b-1* double mutant had a significantly slower
323 circadian clock than Col-0 (Supplemental Fig. S8A), consistent with previously reported
324 redundant roles for *PRP19A* and *PRP19B* in circadian clock regulation (Feke et al., 2019).
325 Similarly, loss of function of other NTC members, including *PRL1*, *CDC5* and *SKIP*, also
326 lengthened the clock period by 1 to 3 hours (Supplemental Fig. S2B; Supplemental Fig. S8B-C),
327 similar to previous reports for *prl1-9* and *skip-1* mutants (Li et al., 2019).

328

329 Since *PRP19* co-purifies with *XCT* (Table 1) and they both control the pace of the circadian
330 clock (Supplemental Fig. S8A), we hypothesized they might function in the same pathway to
331 regulate the clock. To test this hypothesis, we introduced *prp19a-1* and *prp19b-1* mutant alleles,
332 which express greatly decreased and near-null levels of *PRP19A* and *PRP19B*, respectively
333 (Supplemental Fig. S9), into the null *xct-2* background and assayed their circadian clock
334 phenotypes. Interestingly, we found that neither the circadian period of *prp19a-1 xct-2* nor of
335 *prp19b-1 xct-2* was significantly different from Col-0 (Fig. 6A; Supplemental Fig. S10),
336 indicating that both *prp19* mutants can fully suppress the short-period phenotype of *xct-2*.
337 Notably, *prp19a-1* and *prp19b-1* single mutants only have slightly longer circadian periods than
338 Col-0. This suggests that the rescued clock function in *prp19 xct* double mutants is not likely due
339 to additive genetic interactions. Thus, our data show that functional *PRP19A* and *PRP19B* are
340 both necessary for *XCT* in regulation of circadian period.

341
342 To further investigate the functional association between *XCT* and *PRP19*, we next asked
343 whether *prp19* mutants suppress other developmental and physiological defects observed in *xct-2*.
344 In contrast to the circadian period, the reduced rosette size in *xct-2* was not significantly restored
345 in either *prp19a-1 xct-2* or *prp19b-1 xct-2* (Supplemental Fig. S11), indicating that the effects of
346 *XCT* on rosette development and the circadian clock period are genetically separable. This is
347 consistent with our observation that *xct-1* and *xct-2* both have short circadian period phenotypes
348 but only *xct-2* is morphologically different from Col-0 (Supplemental Fig. S1).

349
350 Next, to determine whether suppression of the short clock period phenotype in *xct-2 prp19*
351 mutants is due to reversal of the *xct-2* splicing defects, we conducted qRT-PCR experiments to
352 examine the abundance of *xct*-induced aberrantly-spliced mRNA isoforms of core clock genes in
353 *prp19a-1 xct-2* and *prp19b-1 xct-2*. Surprisingly, none of the aberrantly-spliced isoforms tested
354 showed significantly different abundance in *prp19a-1 xct-2* and *prp19b-1 xct-2* relative to *xct-2*
355 (Fig. 6B-F). Consistent with previous reports for functional redundancy between *PRP19A* and
356 *PRP19B* (Monaghan et al., 2009; Li et al., 2019), we noticed a statistically significant defect in
357 splicing of the third intron of *LNK2* in the *prp19a-1 prp19b-1* double mutant but not the *prp19a-*
358 *1* or *prp19b-1* single mutants. We also checked the expression levels of fully-spliced or total

359 mRNA isoforms of the five core clock genes that are aberrantly-spliced in *xct-2*. In all cases,
360 addition of *prp19a-1* or *prp19b-1* to *xct-2* did not alter the abundance of functionally spliced
361 isoforms of those clock genes (Supplemental Fig. S12). Thus, similar to the developmental
362 defects, the splicing defects of core clock genes are genetically separable from the circadian
363 clock phenotype of *xct-2*.

364

365 Discussion

366 The accurate removal of introns from pre-mRNAs is an essential step of gene expression in all
367 eukaryotes. In this work, we report that *XCT* is a global regulator of pre-mRNA splicing in
368 Arabidopsis. Multiple lines of evidence suggest that orthologs of *XCT* share conserved
369 molecular and cellular functions across kingdoms. Previous mass spectrometry data showed that
370 *FAM50A* and *FAM50B*, two human homologs of *XCT*, physically associate with the affinity-
371 purified spliceosomal C complex (Bessonov et al., 2008; Bessonov et al., 2010). Loss of
372 *FAM50A* function induces transcriptome-wide pre-mRNA splicing defects in both human and
373 zebrafish (Lee et al., 2020). Similarly, a recent study in Arabidopsis also found that *XCT*
374 associates with spliceosomal proteins and regulates splicing (Liu et al., 2022). In this paper, we
375 show that *XCT* physically co-purifies with PRP19 and other NTC-associated proteins (Table 1).
376 Furthermore, our PacBio Iso-Seq data indicate that the efficiency and fidelity of pre-mRNA
377 splicing are negatively impacted in both the partial loss-of-function mutant *xct-1* and the null
378 mutant *xct-2* but are largely restored in *xct-2 XCT* (Fig. 2). Therefore, *XCT* orthologs likely play
379 evolutionarily conserved roles in pre-mRNA splicing. It would be interesting to apply structural
380 biology approaches to further investigate what conserved functional domains among *XCT*
381 homologs might contribute to their splicing activities.

382

383 Studies have shown that intron retention is the most prevalent type of alternative splicing event
384 in Arabidopsis (Wang and Brendel, 2006; Filichkin et al., 2010). Correspondingly, mutations in
385 many Arabidopsis splicing factors mainly cause intron retention (Supplemental Fig. S3; Schlaen
386 et al., 2015; Li et al., 2019). Here we identify *XCT* as an unusual splicing regulator that
387 specifically controls the fidelity of 3' splice site selection (Fig. 2D-E; Fig. 3). Biochemical
388 studies of splicing in yeast revealed that several DEAH-box ATPases are important for the

389 selection of 3' splice sites (Horowitz, 2012). For example, PRP22, a DEAH-box ATPases that
390 co-purifies with XCT (Table 1; Liu et al., 2022), represses usage of aberrant 3' splice sites and
391 promotes spliceosome scanning for downstream alternative 3' splice sites in yeast (Mayas et al.,
392 2006; Semlow et al., 2016). Studies in human showed that hPRP22, FAM50A and FAM50B, are
393 all abundant in the spliceosomal C complex but nearly absent in B and B* complexes (Bessonov
394 et al., 2008; Bessonov et al., 2010; Zhan et al., 2022). This implies that PRP22 and XCT may
395 have evolutionarily conserved interactions during the second transesterification reaction of
396 splicing, when 5' and 3' splice sites are joined (Fig. 1). Intriguingly, we detected decreased
397 fidelity of 3' splice site selection in both *xct-1* and *xct-2* mutants (Fig. 3; Supplemental Fig. S4),
398 which is also observed in yeast *prp22* mutants (Semlow et al., 2016). Therefore, our results
399 imply that XCT may work with PRP22 to control the fidelity of 3' splice site selection. Future
400 research on the biochemical functions of XCT using *in vitro* and *in vivo* systems could help
401 reveal how it controls splicing fidelity.

402
403 Previous microarray and RNAseq studies demonstrated that transcription and splicing of a large
404 proportion of Arabidopsis genes are under circadian clock regulation (Covington and Harmer,
405 2007; Hsu and Harmer, 2012; Romanowski et al., 2020; Yang et al., 2020). Consequently, timing
406 of sample collection is an important consideration in gene expression and splicing analysis,
407 especially when comparing genotypes with different circadian periods. Here we employed a
408 more efficient sampling method by harvesting plants at twelve evenly distributed time points
409 across a day and pooling them before analysis. Our pooling strategy enabled us to detect
410 transcripts of genes with the distribution of peak phases of expression mirroring that of all clock-
411 regulated genes (Fig. 4B; Romanowski et al., 2020). Overall, this strategy allowed us to identify
412 more clock-regulated differentially spliced transcripts in *xct-2* mutants than in a recent study in
413 which plants were collected at a single time point (Liu et al., 2022). For example, we report
414 novel differential splicing events in afternoon-expressed genes including *PRR7* and *TOC1* (Fig.
415 4A; Supplemental Fig. S7C-D). In fact, our time-course qPCR data suggest that abundance of the
416 aberrantly spliced isoforms of these clock-regulated genes fluctuates by over 99% depending on
417 time of sample collection (Fig. 5F-I). Thus, our results demonstrate the advantages of pooling
418 samples when conducting transcriptome-wide splicing analysis of clock-regulated genes.

419

420 Using this strategy, we were able to investigate whether *XCT* preferentially affects splicing at
421 certain times of day. Indeed, we found that dawn-expressed genes are significantly more likely to
422 be mis-spliced in *xct* mutants than those with other peak phases (Fig. 4C-D; Supplemental Fig.
423 S6). This suggests that *XCT* activity in or its association with the spliceosome may be clock-
424 regulated. An alternative explanation for the overrepresented mis-splicing of dawn-expressed
425 genes could be that *cis*-regulatory elements of those genes might preferentially recruit *XCT* to
426 control their splicing. This possibility is supported by previous studies showing that *XCT*
427 orthologs in fission yeast and *Chlamydomonas* are chromatin-associated and in the latter case
428 recruit RNA polymerase II (Pol II) to promoter regions (Anver et al., 2014; Li et al., 2018).

429

430 Alternative splicing regulates various biological processes, including the function of the
431 circadian clock (Hsu and Harmer, 2014; Nolte and Staiger, 2015). In *Arabidopsis*, such
432 regulation is supported by identification of splicing factor mutants that alter circadian clock
433 period length (Shakhmantsir and Sehgal, 2019). Some splicing factors, such as *GEMIN2* and
434 *SICKLE*, interact epistatically with one or more alternatively spliced clock genes in the control of
435 period length (Schlaen et al., 2015; Marshall et al., 2016), suggesting changes in the pace of the
436 clock are due to altered splicing of these clock genes. Whereas in other cases, the mis-regulated
437 circadian period can only be partially attributed to changes in levels of splicing variants of clock
438 genes (Sanchez et al., 2010; Wang et al., 2012). Additionally, in most splicing factor mutants,
439 only small fractions of total transcripts are aberrantly processed (Jones et al., 2012; Perez-
440 Santángelo et al., 2014; Feke et al., 2019; Li et al., 2019). Therefore, whether these small
441 changes in levels of aberrantly spliced isoforms could lead to significantly decreased levels of
442 functional proteins and thereby cause the observed circadian phenotypes remains unclear.

443

444 Here, we demonstrate that in *xct* mutants the circadian clock phenotype is genetically separable
445 from altered levels of aberrantly spliced mRNA variants of core clock gene. We found that loss
446 of *XCT* function accelerates the clock and causes aberrant splicing of five core clock genes
447 (Supplemental Fig. S1; Fig. 4A). Surprisingly, the clock phenotype but not the splicing defects of
448 the five clock genes in *xct-2* is suppressed by reduction of *PRP19A* or *PRP19B* function (Fig. 6).

449 Similarly, the clock in *xct-1* runs slightly faster than *xct-2* but the splicing defects, including the
450 aberrant splicing of *TOC1*, *TIC* and *CCA1*, are more severe in the latter (Fig. 2; Supplemental
451 Fig. S5). Collectively, these data demonstrate that the short period phenotypes and altered levels
452 of clock gene splicing variants are genetically separable in *xct* mutants.

453

454 How *XCT* regulates the pace of the circadian clock is still an outstanding question. Although we
455 argue that changes in levels of aberrantly spliced clock mRNAs are not responsible for the
456 accelerated clock in *xct* mutants, one possibility is that alterations in the overall kinetics of pre-
457 mRNA splicing may cause circadian period phenotypes. Indeed, pharmacological perturbations
458 of global transcription and translation efficiency can both lengthen the circadian period (de Melo
459 et al., 2021; Uehara et al., 2022). Those results suggest that changes in the kinetics of RNA
460 processing might cause the period phenotypes observed in plants mutated for some splicing
461 factors.

462

463 Alternatively, *XCT* may control the circadian clock function independent of its role in pre-
464 mRNA splicing. In *Chlamydomonas*, the *XCT* homolog XAP5 co-immunoprecipitates with
465 RNA Pol II (Li et al., 2018), suggesting that *XCT* orthologs may possess transcriptional
466 regulatory activities. In this paper, we show that NTC components physically and genetically
467 interact with *XCT* to regulate circadian clock period (Table 1; Fig. 6A). Besides splicing, another
468 well-characterized role of the NTC in gene expression is regulation of transcriptional elongation
469 (Chanarat and Sträßer, 2013). Studies in both yeast and *Arabidopsis* have revealed that multiple
470 NTC members, including PRP19, PRL1 and CDC5, physically associate with RNA Pol II and
471 participate in transcript elongation (Chanarat et al., 2011; Zhang et al., 2013; Zhang et al., 2014).
472 In addition, the NTC component SKIP interacts with Polymerase-Associated Factor 1 complex
473 to regulate transcription in a splicing-independent manner (Li et al., 2019). Interestingly, a recent
474 study showed that inhibition of transcriptional elongation by decreasing phosphorylation of the
475 RNA Pol II C-terminal domain lengthens circadian period in *Arabidopsis* (Uehara et al., 2022). It
476 is therefore possible that *XCT* affects circadian period by altering transcriptional elongation.

477

478 Yet another possibility is that *XCT* affects a cellular process independently of its role in gene
479 expression. For example, PRP19 is known to facilitate DNA repair by its E3 ubiquitin ligase
480 activity independent of its involvement in the spliceosomal complex (Maréchal et al., 2014;
481 Idrissou and Maréchal, 2022). Indeed, there is increasing evidence that many RNA binding
482 proteins directly participate in DNA double-strand break responses (Klaric et al., 2021). A recent
483 study showed that the NTC-associated protein MOS4-ASSOCIATED COMPLEX SUBUNIT
484 5A (MAC5A) physically interacts with the 26S proteasome and regulates its activities in
485 response to DNA damage (Meng et al., 2022). Intriguingly, we recently reported that loss of *XCT*
486 function also disturbs the DNA damage response pathway (Kumimoto et al., 2021). Thus, it is
487 possible that *XCT* works with *PRP19* in this pathway separately from its role in RNA processing.
488 Future research is required to understand the nature of the relationship of between *XCT* and the
489 NTC in the control of circadian clock function and other essential biological processes.

490

491 **Materials and Methods**

492 **Plant materials and growth conditions**

493

494 All *Arabidopsis thaliana* plants used in this study are Columbia-0 (Col-0) ecotype and contain a
495 *CCR2::LUC* reporter for circadian clock assays. The *xct-1*, *xct-2*, *xct-2 pXCT::gXCT-YFP-HA*,
496 *prp19a-1*, *prp19b-1*, *prl1-2*, *cdc5-1* and *skip-1* genotypes have been previously described
497 (Martin-Tryon and Harmer, 2008; Monaghan et al., 2009; Zhang et al., 2014; Wang et al., 2012).
498 All the double mutants in this study were produced by crossing. Unless otherwise specified,
499 seeds were surface sterilized with chlorine gas for 3 hours (50 ml 100% bleach + 3ml 1M HCl)
500 and then plated on 1x Murashige and Skoog (MS) growth media containing 0.7% agar, pH 5.7.
501 After 3d stratification in dark at 4°C, plates were transferred to 12-h light (cool white fluorescent
502 bulbs, 55 $\mu\text{mol m}^{-2} \text{s}^{-1}$) / 12-h dark cycles at 22°C for a variable number of days depending on the
503 experiment.

504

505 **Immunoprecipitations and mass spectrometry**

506

507 Plants were grown in 12-h light / 12-h dark cycles and harvested on day 10 at ZT3 or ZT17.
508 Approximately 7.5g of vegetative tissue was flash frozen in liquid nitrogen and ground into fine
509 powder with a mortar and pestle. Ground tissue was resuspended in nuclei enrichment buffer (50
510 mM Tris pH7.5, 400 mM sucrose, 2.5 mM MgCl₂, 1 mM DTT, 1 mM PMSF, cOmplete Protease
511 Inhibitor cocktail (Roche)), the nuclear pellet was collected, resuspended in IP buffer (100mM
512 Tris pH7.5, 1mM EDTA, 75mM NaCl, 10% glycerol, 0.3% Triton X-100, 0.05% SDS, 10 mM
513 MG-132, 1 mM PMSF, , cOmplete Protease Inhibitor cocktail (Roche)) and pelleted again.
514 Nuclei were resuspended in IP buffer, disrupted via sonication, and adjusted to 1 mg/mL in IP
515 buffer. 1 mg of extract was incubated with μ MACS MicroBeads conjugated to an anti-HA
516 monoclonal antibody (Miltenyi Biotec) and beads were then captured on μ MACS M-columns.
517 Beads were washed 3x with ice cold IP buffer and 1x with ice cold TE buffer (10 mM Tris-HCl
518 pH 8.0, 0.1 mM EDTA). Proteins were eluted off the beads with elution buffer (Miltenyi Biotec).
519 Proteins were resolved using SDS polyacrylamide gel electrophoresis and gels were sent to the
520 Rutgers Biological Mass Spectrometry Facility, Robert Wood Johnson Medical School. Proteins
521 were eluted and subjected to mass spectrometry as previously described (Wei et al., 2020).

522

523 **PacBio Iso-Seq and bioinformatic analysis**

524

525 Arabidopsis seeds were surface sterilized in 70% ethanol prepared in 0.1% (v/v) Triton X-100
526 (Sigma) for 5 minutes and then in 100% Ethanol for 20 minutes. After air drying, seeds were
527 plated on 1x MS growth media containing 0.7% agar. After cold stratification for 3 days, plates
528 were transferred to constant light (55 μ mol m⁻² s⁻¹) and temperature (22°C). Approximately 60
529 mg of whole seedlings of each genotype were collected every 2h over 24 hours on day 11 and
530 pooled as indicated in Fig. 2A. Three biological replicates were collected for each genotype.
531 Samples were flash-frozen in liquid nitrogen, and ground into fine powder using a beadbeater.
532 Total RNA was extracted using an RNeasy Plant Mini Kit (Qiagen) followed by purification
533 using the RNA Clean & Concentrator Kit (Zymo Research). Purified RNAs were quantified
534 using a Nanodrop (ThermoFisher) and quality control was performed by an Agilent Bioanalyzer
535 2100. All samples had a 260/230 nm ratio higher than 1.9, 260/280nm ratio between 2 and 2.15,
536 and RIN score higher than 8. PacBio Sequel II library preparation and RNA-sequencing (Iso-Seq)

537 was performed by UC Davis DNA Technologies & Expression Analysis Core
538 (<https://dnatech.genomecenter.ucdavis.edu/pacbio-library-prep-sequencing/>).

539
540 Raw reads generated by the PacBio Sequel II sequencer were imported into PacBio SMRT Link
541 v 8.0 for Circular Consensus Sequence (CCS) calling and demultiplexing. Next, poly(A) tails
542 and concatemers were removed using the refine command from isoseq3 package via Bioconda (v
543 3.10) with the option ‘--require-polya’. Then the fastq files containing full-length non-
544 concatemer reads were mapped to Arabidopsis TAIR 10 genome assembly using minimap2 (v
545 2.17) with the parameter ‘-ax splice -t 30 -uf --secondary=no -C5’. For differential splicing
546 analysis, counts of exonic regions and known/novel splice junctions were generated using
547 QoRTs software package (v 1.3.6) (Hartley and Mullikin, 2015) with the parameter ‘--stranded --
548 singleEnded --stranded_fr_secondstrand --keepMultiMapped’. To adapt to the long-read data,
549 the ‘maxPhredScore’ was set to 93 and the ‘maxReadLength’ was adjusted manually for each
550 library. To increase the power of detecting novel splice junctions, the ‘--minCount’ threshold was
551 set to 5. The raw count data was then loaded to JunctionSeq R package (v 1.5.4) (Hartley and
552 Mullikin, 2016) to determine differential usage of exons or splice junctions relative to the overall
553 expression of the corresponding gene with a false discovery rate (FDR) of 0.05. Genes with at
554 least one differentially spliced exon/junction were compared to the total circadian-clock-
555 regulated genes (Romanowski et al., 2020) as described in Fig. 4.

556

557 **RNA extraction and RT-PCR**

558

559 For time-course qRT-PCR analysis, Arabidopsis seedlings were entrained in 12-h light / 12-h
560 dark cycles for 9 days before transferred to constant light and temperature ($55 \mu\text{mol m}^{-2} \text{s}^{-1}$,
561 22°C). Starting from day 9, approximately 15-20 whole seedlings of each genotype were
562 harvested every 4h over the 72-h period. For single time point gene expression and splicing
563 analysis, 10-d-old seedlings grown in 12-h light / 12-h dark cycles at 22°C were harvested at
564 estimated peak time of expression for each studied gene. Collected tissue was immediately
565 frozen in liquid nitrogen and ground into fine powder using a beadbeater. Total RNA was
566 isolated using TRIzol reagent (Invitrogen) and quantified with a Nanodrop (ThermoFisher). 200

567 ng of total RNA was used for cDNA synthesis with an oligo(dT)18 primer and SuperScriptIII
568 (Invitrogen) reverse transcriptase. Diluted cDNAs were used as templates for qRT-PCR and
569 semi-qRT-PCR reactions. The qRT-PCR was carried out as previously described (Martin-Tryon
570 et al., 2007) using a Bio-Rad CFX96 thermocycler. Primers amplifying the aberrantly spliced or
571 total transcripts were tested by standard curve and melt curve assays. Relative expression ($\Delta\Delta Cq$)
572 values were normalized to the geometric mean of *PROTEIN PHOSPHATASE 2a (PP2A)* and
573 *ISOPENTENYL DIPHOSPHATE ISOMERASE 2 (IPP2)* expression levels. For semi-qRT-PCR,
574 splice-junction specific primer pairs were designed to amplify regions flanking the aberrantly
575 spliced introns of interest. The size and abundance of the resultant PCR products were then
576 analyzed and quantified by LabChip GX bioanalyzer (PerkinElmer). The expression analyses
577 represent two to three biological replicates. All primers used in this study are described in
578 Supplemental Dataset S5.

579

580 **Circadian period analysis**

581

582 After growing on MS plates under 12-h light / 12-h dark cycles for 6 days, Arabidopsis seedlings
583 were sprayed with 3 mM D-luciferin (Biosynth) prepared in 0.01% (v/v) Triton X-100 (Sigma)
584 and then transferred to a growth chamber with a constant 22°C and constant light provided by red
585 and blue LED SnapLites (Quantum Devices, 35 $\mu\text{mol m}^{-2} \text{s}^{-1}$ each) for imaging. Luciferase
586 activity was detected using a cooled CCD camera (DU434-BV [Andor Technology]).

587 Bioluminescence signals from the images were quantified using MetaMorph 7.7.1.0 software
588 (Molecular Devices). Subsequent circadian period estimation and rhythmicity analysis were
589 performed using Biological Rhythms Analysis Software System 3.0 (BRASS) by fitting the
590 bioluminescence data to a cosine wave through Fourier Fast Transform-Non-Linear Least
591 Squares (Plautz et al., 1997).

592

593 **Rosette size measurement**

594

595 Seeds on MS plates were germinated in a growth chamber with 12-h light / 12-h dark cycles at a
596 constant 22°C. 15-day-old seedlings were transferred to soil and grown in 16-h light (cool-white

597 fluorescent bulbs, 75 $\mu\text{mol m}^{-2} \text{s}^{-1}$) / 8-h dark long day condition at a constant 22°C. Rosette sizes
598 of 39-day-old plants were determined by the greatest distance between rosette leaves using a
599 digital caliper.

600

601 **Accession Numbers**

602

603 All the *Arabidopsis thaliana* genes studied in this paper can be found under the following
604 accession numbers:

605 *XCT*, AT2G21150

606 *PRP19A*, AT1G04510

607 *PRP19B*, AT2G33340

608 *PRL1*, AT4G15900

609 *SKIP*, AT1G77180

610 *CDC5*, AT1G09770

611 *LHY*, AT1G01060

612 *LNK2*, AT3G54500

613 *TIC*, AT3G22380

614 *PRR7*, AT5G02810

615 *TOC1*, AT5G61380

616 *SPPA*, AT1G73990

617 *IPP2*, AT3G02780

618 *PP2A*, AT1G69960

619 *CCA1*, AT2G46830

620

621 **Data Availability**

622

623 All our MS data were deposited and available at Center for Computational Mass Spectrometry
624 (CCMS, Dataset: MSV000090830). Our PacBio Iso-Seq data were deposited and available in
625 NCBI Gene Expression Omnibus (GEO, Accession number: GSE220902).

626

656

657

658 Funding

659

660 This work was supported by awards from the National Institutes of Health (R01 GM069418 to
661 SLH) and the United States Department of Agriculture-National Institute of Food and
662 Agriculture (CA-D-PLB-2259-H to SLH). HZ was supported by a fellowship from China
663 Scholarship Council (CSC #201806010204 to HZ).

664

665 Acknowledgments

666

667 We thank the Arabidopsis Biological Resource Center for providing seeds. We thank Haiyan
668 Zheng and the Biological Mass Spectrometry Facility of Robert Wood Johnson Medical School
669 and Rutgers for mass spectrometry analysis. They are supported by NIH Shared Instrumentation
670 Grant S10OD01640. We thank the DNA Technologies and Expression Analysis Core at the UC
671 Davis Genome Center for performing PacBio Iso-Seq experiment. They are supported by NIH
672 Shared Instrumentation Grant 1S10OD010786-01. We thank Julin Maloof for statistical advice,
673 as well as members of the Harmer, Maloof, and Shabek labs for helpful discussions.

674

675

676

677 Figure Legends

678

679 **Figure 1. Simplified overview of pre-mRNA splicing reactions.** A schematic diagram
680 highlighting the two catalytic transesterification steps and the association between the NTC and
681 the spliceosomal complex during pre-mRNA splicing. Gray boxes and solid black lines represent
682 exons and introns, respectively. U1-U6 small nuclear ribonucleoproteins (snRNPs) are indicated
683 by yellow circles. The NTC is indicated by a green oval.

684

685 **Figure 2. Transcriptome-wide analysis reveals *XCT* as a global pre-mRNA splicing**
 686 **regulator.** A, Experimental design and sampling method for the PacBio Iso-Seq experiment.
 687 White and grey boxes represent subjective day and subjective night, respectively. Arabidopsis
 688 seedlings were grown at constant light and temperature for 10 days before being harvested and
 689 pooled. B and C, Numbers of differentially enriched splicing events represented by significantly
 690 differentially down- (B) or up-regulated (C) splice junctions in *xct-1*, *xct-2* and *xct-2*
 691 complemented with p*XCT*::g*XCT*-*YFP*-*HA* compared with Col-0 (false discovery rate < 0.05). D
 692 and E, Frequency of different classes of 5' and 3' splice sites among down- (D) or up-regulated
 693 (E) splice junctions in *xct-1* and *xct-2*. Known or novel 5' and 3' splice sites were classified by
 694 comparison to TAIR10 genome annotation.

695
 696 **Figure 3. *XCT* is required for the fidelity of 3' splice site selection during pre-mRNA**
 697 **splicing.** A, A schematic diagram showing the structure of a typical U2-type splice junction. Y:
 698 pyrimidine. B, Distribution of the distance between each pair of novel 3' splice site and its
 699 corresponding canonical 3' splice sites in *xct-2*. C, Pictograms showing the frequency of
 700 nucleotides in the 23-mers sequences flanking the 3' splice sites in all expressed, down-regulated
 701 and up-regulated splice junctions in *xct-2*. D, Maximum Entropy Model scores showing the
 702 strength of 3' splice sites of all expressed, down-regulated and up-regulated junctions in *xct-2*. E,
 703 Percentage of pyrimidines at the -3 position (i.e. the nucleotide preceding the AG at 3' splice
 704 site) in *xct-2*. F, Counts of pyrimidines in the Y10 polypyrimidine tract upstream of the 3' splice
 705 sites in *xct-2*. PPT, polypyrimidine tract. The lines in the boxplot represent the 75% quartile,
 706 median and 25% quartile of the data, respectively. Statistical significance in (D) and (F) was
 707 determined using linear regression model with junction class as a fixed effect and is shown in
 708 lower case letters (Tukey's multiple comparison test, $P < 0.05$). Statistical significance in (E) was
 709 determined by Fisher's exact test: **: $P < 0.01$; ***: $P < 0.001$.

710
 711 **Figure 4. Dawn-phased genes are significantly enriched among all the circadian-clock-**
 712 **regulated genes that are aberrantly spliced in *xct-2*.** A, Venn diagram showing the overlaps of
 713 aberrantly spliced genes in *xct-1*, *xct-2*, and total circadian-clock-regulated genes (Romanowski
 714 et al., 2020). The core circadian clock genes that are mis-spliced in both *xct* mutants are indicated

715 in red (non-clock-regulated) and blue (clock-regulated) fonts. Only genes considered as
 716 ‘detected’ in all three RNA-Seq datasets are included. B and C, Phases of estimated peak
 717 expression of all circadian clock-regulated genes (Romanowski et al., 2020) that are detected (B)
 718 or significantly aberrantly spliced (C) in *xct-2* grouped in 2-hour bins. The white and gray
 719 backgrounds represent the subjective day and subjective night, respectively. Sizes of blue sectors
 720 depict number of transcripts per 2-hour time interval. D, Times of day with a significantly higher
 721 ratio of the number of aberrantly spliced transcripts in *xct-2* (C) to all clock-regulated transcripts
 722 (B) than expected by chance. Sizes of green sectors depict *P*-values (Fisher’s exact test).

723

724 **Figure 5. Time-course qRT-PCR experiments validate the role of *XCT* in regulating pre-**
 725 **mRNA splicing of clock-regulated and non-clock-regulated genes.** A - E, Sashimi plots
 726 showing PacBio Iso-Seq reads mapped to *LHY* (A), *LNK2* (B), *PRR7* (C), *TOC1* (D) and *SPPA*
 727 (E) in Col-0 (teal), *xct-2* (orange) and *xct-2 XCT* (purple). The red rectangles highlight the
 728 aberrantly spliced exon-exon junctions that are examined by qRT-PCR in (F) - (J). F - J,
 729 Normalized expression of the aberrantly spliced isoforms of *LHY* (F), *LNK2* (G), *PRR7* (H),
 730 *TOC1* (I) and *SPPA* (J) in Col-0, *xct-2* and *xct-2 XCT*. Samples were collected every four hours
 731 over a 72-h window. Expression levels were examined by qRT-PCR using splice-junction-
 732 specific primers and normalized to *PP2A* and *IPP2*. Data points represent mean \pm se from three
 733 independent biological replicates. For each isoform in each biological replicate, the normalized
 734 expression levels were relative to the highest expression levels of their total transcripts in Col-0
 735 across all time points. Teal lines, wild type Col-0; orange lines, *xct-2* mutants; purple lines, *xct-2*
 736 *XCT*. Black background, dark period; white and gray background, light period during subjective
 737 day and night, respectively.

738

739 **Figure 6. Loss of *PRP19* function suppresses the short circadian clock period phenotype**
 740 **but not the splicing defects of core clock genes in *xct-2*.** A, Circadian periods of Col-0, *xct-2*,
 741 *prp19a-1*, *prp19b-1*, *prp19a-1 prp19b-1*, *prp19a-1 xct-2* and *prp19b-1 xct-2* plants. B - F,
 742 Normalized expression of the aberrantly spliced isoforms of *LHY*, *LNK2*, *TIC*, *PRR7* and *TOC1*
 743 in Col-0, *xct-2*, *prp19a-1*, *prp19b-1*, *prp19a-1 prp19b-1*, *prp19a-1 xct-2* and *prp19b-1 xct-2*.
 744 Samples were collected at the estimated peak expression time for each gene. Expression levels

745 were examined by qRT-PCR using splice-junction-specific primers and normalized to *PP2A* and
 746 *IPP2*. Data points represent mean \pm se from two independent biological replicates. Statistical
 747 significance was determined using linear regression model with genotype as a fixed effect and is
 748 shown in lower case letters (Tukey's multiple comparison test, $P < 0.05$).

749

750 **Table 1. XCT physically associates with splicing-related proteins, especially the NTC**
 751 **components, in Arabidopsis.** Mass Spectrometry (MS) data showing that spliceosome-
 752 associated proteins are significantly more enriched in XCT-YFP-HA-IP than control IP (fold
 753 enrichment > 3 ; P -value < 0.05 , Welch two sample t.test). The full list of proteins co-purified
 754 with XCT are described in Supplemental Dataset S1. Only proteins detected in each biological
 755 replicate and with 20 or more total peptides counts are shown. n.a., data not available.

AGI	<i>A. thaliana</i> protein name	<i>P</i> -value	Fold enrichment	Category	<i>S. cerevisiae</i> homolog	<i>H. sapiens</i> homolog
AT2G21150	XCT	6.21E-04	Inf	n.a.	n.a.	FAM50A
AT1G04510	PRP19A/MAC3A/PUB59	1.52E-02	4.2	NTC	Prp19p	PRPF19/PSO4/SNEK1
AT2G33340	PRP19B/MAC3B/PUB60	2.17E-03	4.8	NTC		
AT4G15900	PRL1/MAC2	1.24E-02	7.7	NTC	Prp46p	PLRG1
AT1G77180	SKIP/MAC6	1.36E-03	4.9	NTC	Prp45p	SNW1
AT1G09770	CDC5/MAC1	4.06E-03	6.7	NTC	Cef1p	CDC5L
AT1G07360	MAC5A	2.15E-03	8.8	NTC	Ecm2p	RBM22
AT5G41770	CRNK1/MAC10	5.78E-03	7.7	NTC	Clf1p/Syf3p	CRNKL1/SYF3
AT3G18790	ISY1/MAC8	1.26E-03	6.1	NTC	Isy1p	ISY1
AT2G38770	EMB2765/MAC7	1.36E-02	4.4	NTC	Cwf11p	AQR
AT5G28740	n.a.	8.86E-03	4.6	NTC	Syf1p	XAB2
AT3G18165	MOS4	4.09E-03	4.5	NTC	Snt309p	BCAS2/SPF27
AT5G51280	n.a.	1.65E-02	4.3	other splicing	Dbp2p	DDX41
AT2G47640	SMD2A	4.93E-03	4.3	other splicing	Smd2p	SNRPD2
AT3G26560	n.a.	8.15E-03	24	other splicing	Prp22p	DHX8
AT1G09760	U2A'	3.51E-02	3.3	U2 complex	Lea1p	SNRPA1

756

757 **References**

758

759 **Anver S, Roguev A, Zofall M, Krogan NJ, Grewal SIS, Harmer SL** (2014) Yeast X-
760 chromosome-associated protein 5 (Xap5) functions with H2A.Z to suppress aberrant
761 transcripts. *EMBO Rep* **15**: 894–902

762 **Bessonov S, Anokhina M, Krasauskas A, Golas MM, Sander B, Will CL, Urlaub H, Stark**
763 **H, Lührmann R** (2010) Characterization of purified human Bact spliceosomal
764 complexes reveals compositional and morphological changes during spliceosome
765 activation and first step catalysis. *RNA* **16**: 2384–2403

766 **Bessonov S, Anokhina M, Will CL, Urlaub H, Lührmann R** (2008) Isolation of an active step
767 I spliceosome and composition of its RNP core. *Nature* **452**: 846–850

768 **Chanarat S, Seizl M, Strässer K** (2011) The Prp19 complex is a novel transcription elongation
769 factor required for TREX occupancy at transcribed genes. *Genes Dev* **25**: 1147–1158

770 **Chanarat S, Sträßer K** (2013) Splicing and beyond: the many faces of the Prp19 complex.
771 *Biochim Biophys Acta* **1833**: 2126–2134

772 **Clough SJ, Bent AF** (1998) Floral dip: a simplified method for *Agrobacterium*-mediated
773 transformation of *Arabidopsis thaliana*. *Plant J* **16**: 735–743

774 **Covington MF, Harmer SL** (2007) The circadian clock regulates auxin signaling and responses
775 in *Arabidopsis*. *PLoS Biol* **5**: e222

776 **Creux N, Harmer S** (2019) Circadian Rhythms in Plants. *Cold Spring Harb Perspect Biol* **11**:
777 a034611

778 **Deng X, Lu T, Wang L, Gu L, Sun J, Kong X, Liu C, Cao X** (2016) Recruitment of the
779 NineTeen Complex to the activated spliceosome requires AtPRMT5. *Proc Natl Acad Sci*
780 *U S A* **113**: 5447–5452

- 781 **Fang X, Shi Y, Lu X, Chen Z, Qi Y** (2015) CMA33/XCT Regulates Small RNA Production
782 through Modulating the Transcription of Dicer-Like Genes in Arabidopsis. *Mol Plant* **8**:
783 1227–1236
- 784 **Feke A, Liu W, Hong J, Li M-W, Lee C-M, Zhou EK, Gendron JM** (2019) Decoys provide a
785 scalable platform for the identification of plant E3 ubiquitin ligases that regulate
786 circadian function. *Elife* **8**: e44558
- 787 **Filichkin SA, Priest HD, Givan SA, Shen R, Bryant DW, Fox SE, Wong W-K, Mockler TC**
788 (2010) Genome-wide mapping of alternative splicing in Arabidopsis thaliana. *Genome*
789 *Res* **20**: 45–58
- 790 **Harmer SL** (2009) The circadian system in higher plants. *Annu Rev Plant Biol* **60**: 357–377
- 791 **Hartley SW, Mullikin JC** (2016) Detection and visualization of differential splicing in RNA-
792 Seq data with JunctionSeq. *Nucleic Acids Res* **44**: e127
- 793 **Hartley SW, Mullikin JC** (2015) QoRTs: a comprehensive toolset for quality control and data
794 processing of RNA-Seq experiments. *BMC Bioinformatics* **16**: 224
- 795 **Hatakeyama S, Yada M, Matsumoto M, Ishida N, Nakayama KI** (2001) U box proteins as a
796 new family of ubiquitin-protein ligases. *J Biol Chem* **276**: 33111–33120
- 797 **Hogg R, McGrail JC, O’Keefe RT** (2010) The function of the NineTeen Complex (NTC) in
798 regulating spliceosome conformations and fidelity during pre-mRNA splicing. *Biochem*
799 *Soc Trans* **38**: 1110–1115
- 800 **Horowitz DS** (2012) The mechanism of the second step of pre-mRNA splicing. Wiley
801 *Interdiscip Rev RNA* **3**: 331–350
- 802 **Hsu PY, Harmer SL** (2012) Circadian phase has profound effects on differential expression
803 analysis. *PLoS One* **7**: e49853

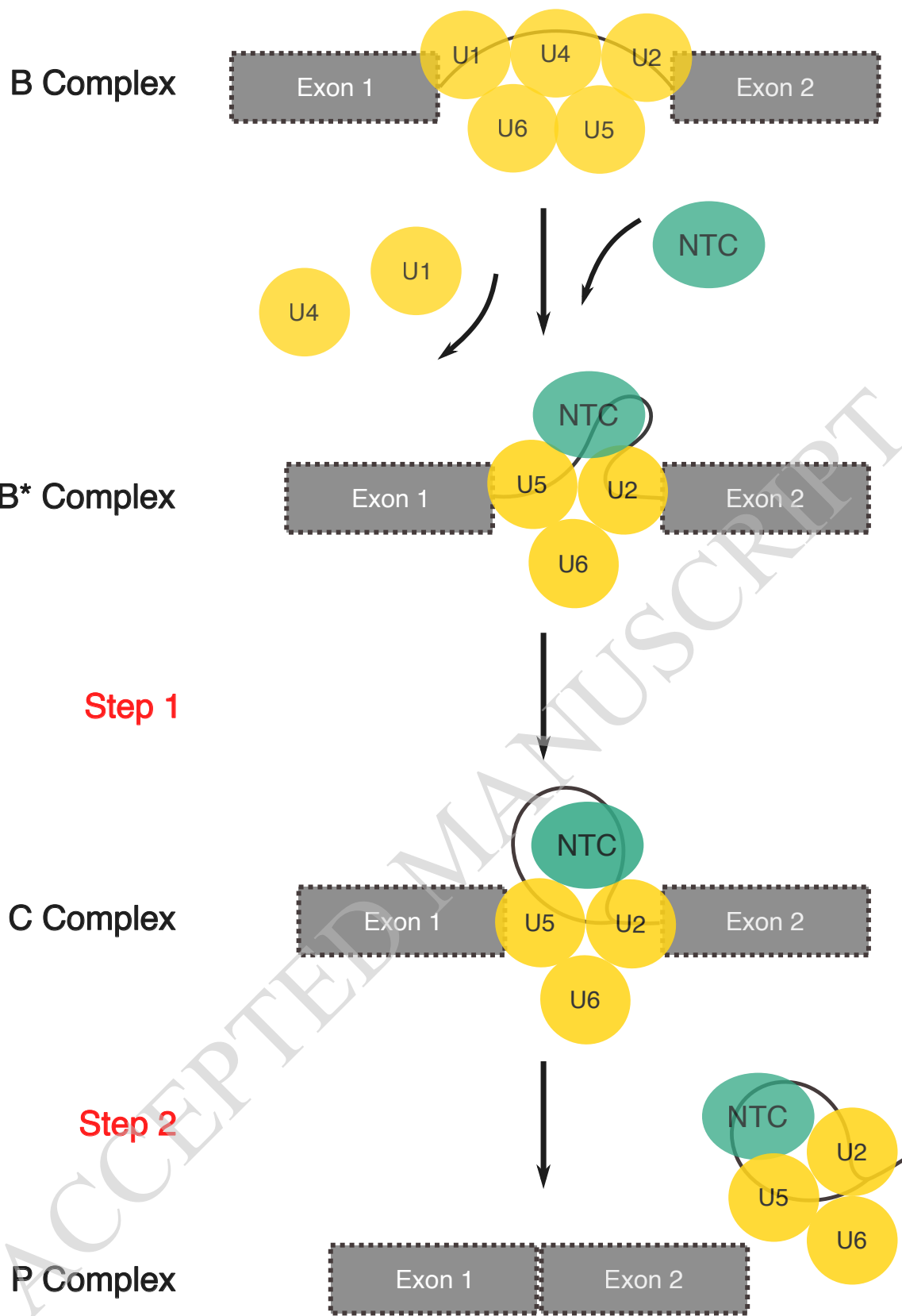
- 804 **Hsu PY, Harmer SL** (2014) Wheels within wheels: the plant circadian system. *Trends Plant Sci*
805 **19**: 240–249
- 806 **Idrissou M, Maréchal A** (2022) The PRP19 Ubiquitin Ligase, Standing at the Cross-Roads of
807 mRNA Processing and Genome Stability. *Cancers (Basel)* **14**: 878
- 808 **James AB, Syed NH, Bordage S, Marshall J, Nimmo GA, Jenkins GI, Herzyk P, Brown**
809 **JWS, Nimmo HG** (2012) Alternative splicing mediates responses of the Arabidopsis
810 circadian clock to temperature changes. *Plant Cell* **24**: 961–981
- 811 **Jia T, Zhang B, You C, Zhang Y, Zeng L, Li S, Johnson KCM, Yu B, Li X, Chen X** (2017)
812 The Arabidopsis MOS4-Associated Complex Promotes MicroRNA Biogenesis and
813 Precursor Messenger RNA Splicing. *Plant Cell* **29**: 2626–2643
- 814 **Jones MA, Williams BA, McNicol J, Simpson CG, Brown JWS, Harmer SL** (2012) Mutation
815 of Arabidopsis spliceosomal timekeeper locus1 causes circadian clock defects. *Plant Cell*
816 **24**: 4066–4082
- 817 **Klaric JA, Wüst S, Panier S** (2021) New Faces of old Friends: Emerging new Roles of RNA-
818 Binding Proteins in the DNA Double-Strand Break Response. *Front Mol Biosci* **8**:
819 668821
- 820 **Koncz C, Dejong F, Villacorta N, Szakonyi D, Koncz Z** (2012) The spliceosome-activating
821 complex: molecular mechanisms underlying the function of a pleiotropic regulator. *Front*
822 *Plant Sci* **3**: 9
- 823 **Kumimoto RW, Ellison CT, Toruño TY, Bak A, Zhang H, Casteel CL, Coaker G, Harmer**
824 **SL** (2021) XAP5 CIRCADIAN TIMEKEEPER Affects Both DNA Damage Responses
825 and Immune Signaling in Arabidopsis. *Front Plant Sci* **12**: 707923
- 826 **Kwon Y-J, Park M-J, Kim S-G, Baldwin IT, Park C-M** (2014) Alternative splicing and
827 nonsense-mediated decay of circadian clock genes under environmental stress conditions
828 in Arabidopsis. *BMC Plant Biol* **14**: 136

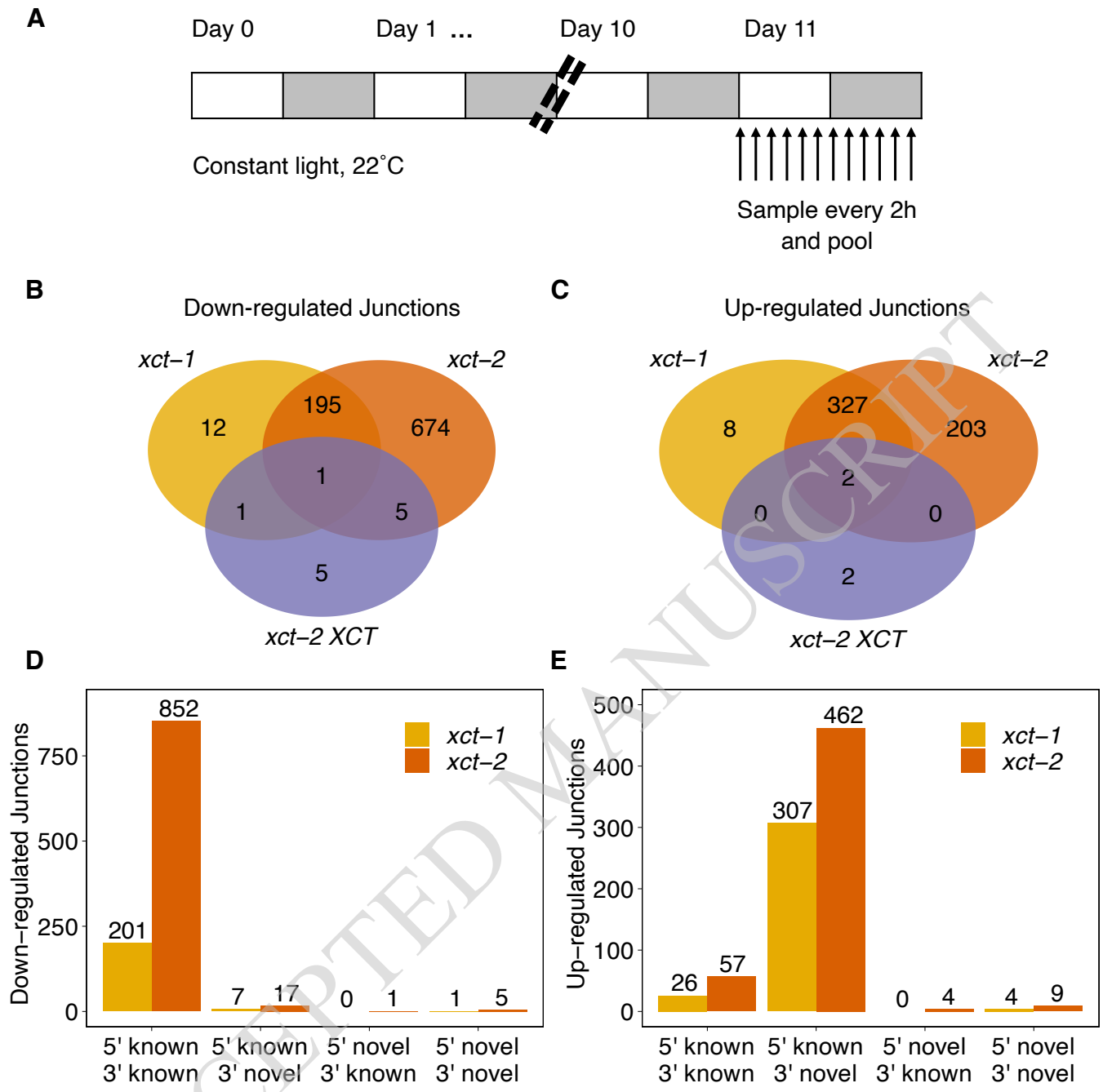
- 829 **Lee Y-R, Khan K, Armfield-Uhas K, Srikanth S, Thompson NA, Pardo M, Yu L, Norris**
830 **JW, Peng Y, Gripp KW, et al** (2020) Mutations in FAM50A suggest that Armfield
831 XLID syndrome is a spliceosomopathy. *Nat Commun* **11**: 3698
- 832 **Li L, Tian G, Peng H, Meng D, Wang L, Hu X, Tian C, He M, Zhou J, Chen L, et al** (2018)
833 New class of transcription factors controls flagellar assembly by recruiting RNA
834 polymerase II in *Chlamydomonas*. *Proc Natl Acad Sci U S A* **115**: 4435–4440
- 835 **Li Y, Yang J, Shang X, Lv W, Xia C, Wang C, Feng J, Cao Y, He H, Li L, et al** (2019) SKIP
836 regulates environmental fitness and floral transition by forming two distinct complexes in
837 *Arabidopsis*. *New Phytol* **224**: 321–335
- 838 **Liu L, Li X, Yuan L, Zhang G, Gao H, Xu X, Zhao H** (2022) XAP5 CIRCADIAN
839 TIMEKEEPER specifically modulates 3' splice site recognition and is important for
840 circadian clock regulation partly by alternative splicing of LHY and TIC. *Plant Physiol*
841 *Biochem* **172**: 151–157
- 842 **Maréchal A, Li J-M, Ji XY, Wu C-S, Yazinski SA, Nguyen HD, Liu S, Jiménez AE, Jin J,**
843 **Zou L** (2014) PRP19 transforms into a sensor of RPA-ssDNA after DNA damage and
844 drives ATR activation via a ubiquitin-mediated circuitry. *Mol Cell* **53**: 235–246
- 845 **Marshall CM, Tartaglio V, Duarte M, Harmon FG** (2016) The *Arabidopsis* sickle Mutant
846 Exhibits Altered Circadian Clock Responses to Cool Temperatures and Temperature-
847 Dependent Alternative Splicing. *Plant Cell* **28**: 2560–2575
- 848 **Martin-Tryon EL, Harmer SL** (2008) XAP5 CIRCADIAN TIMEKEEPER coordinates light
849 signals for proper timing of photomorphogenesis and the circadian clock in *Arabidopsis*.
850 *Plant Cell* **20**: 1244–1259
- 851 **Martin-Tryon EL, Kreps JA, Harmer SL** (2007) GIGANTEA acts in blue light signaling and
852 has biochemically separable roles in circadian clock and flowering time regulation. *Plant*
853 *Physiol* **143**: 473–486

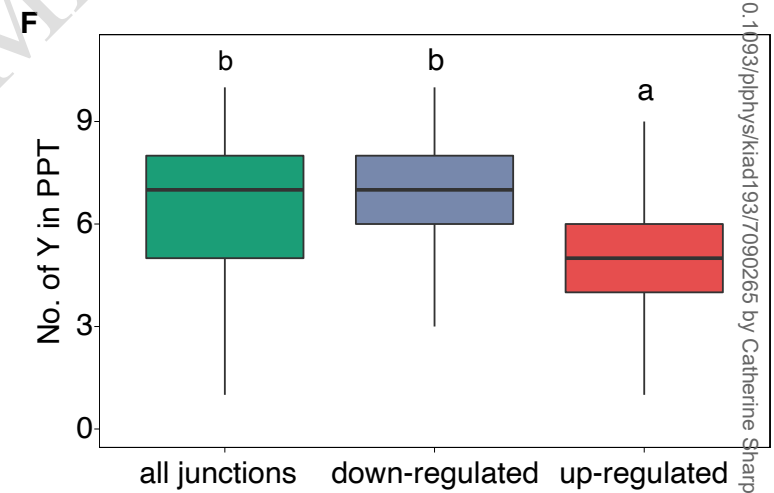
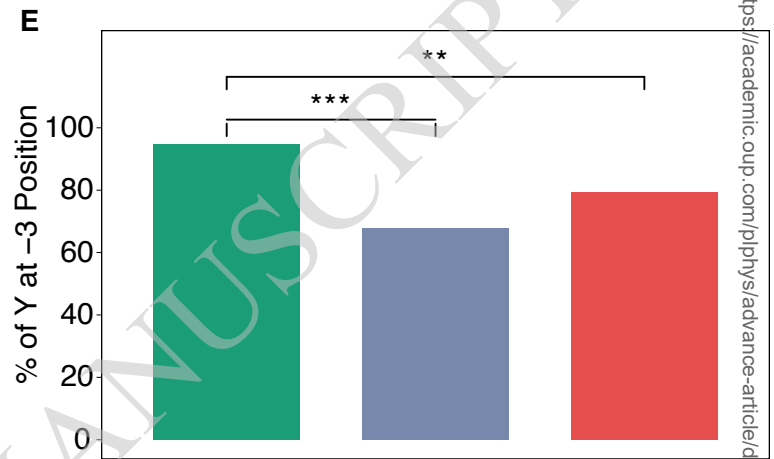
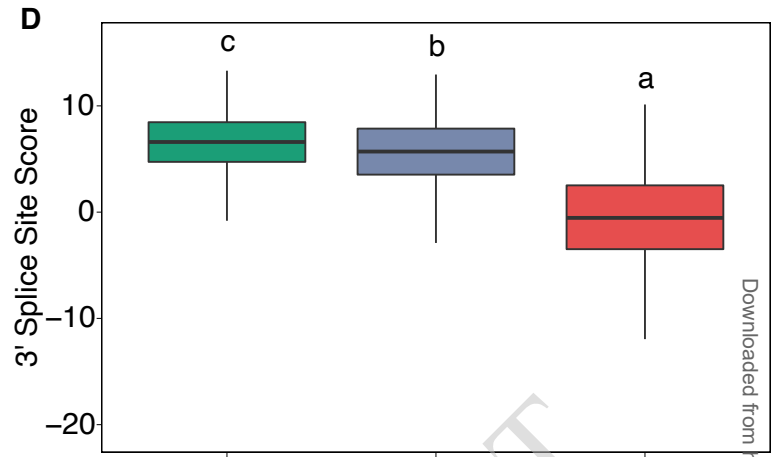
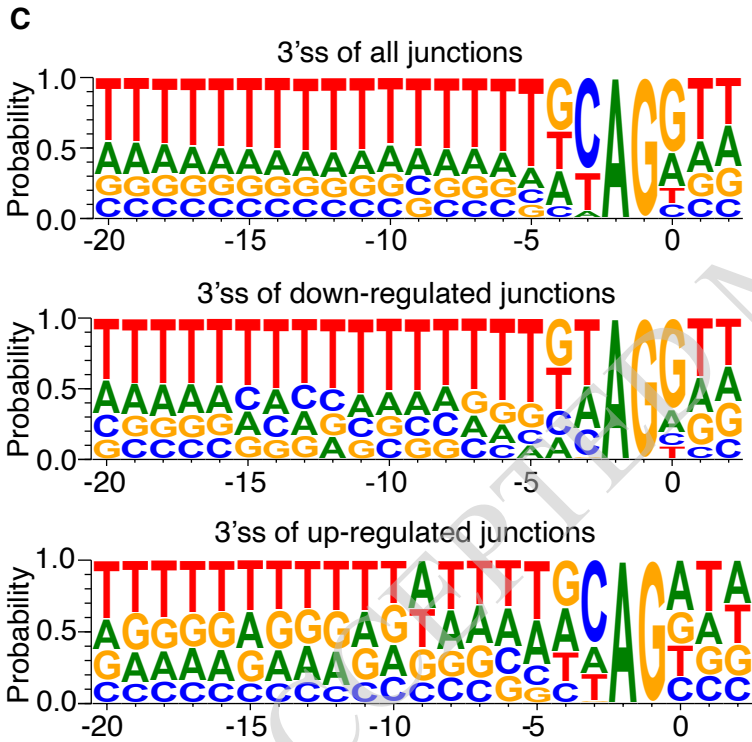
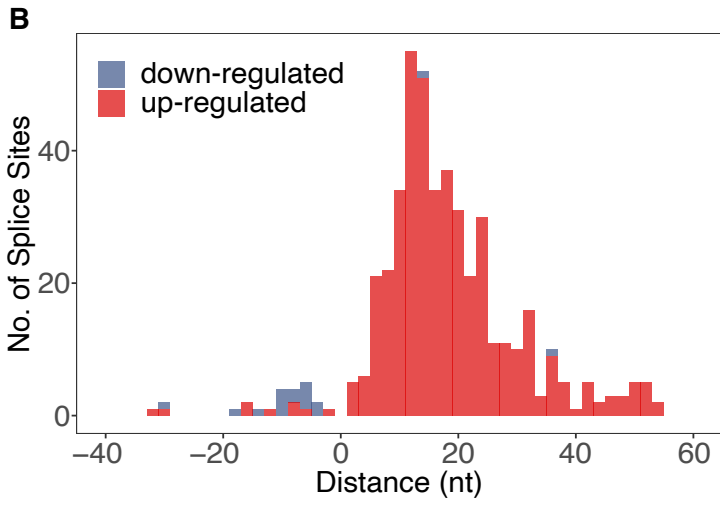
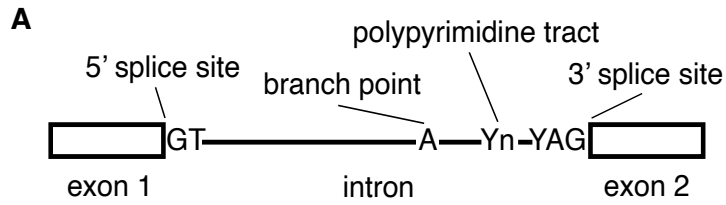
- 854 **Mayas RM, Maita H, Staley JP** (2006) Exon ligation is proofread by the DExD/H-box ATPase
855 Prp22p. *Nat Struct Mol Biol* **13**: 482–490
- 856 **de Melo JRF, Gutsch A, Caluwé TD, Leloup J-C, Gonze D, Hermans C, Webb AAR,**
857 **Verbruggen N** (2021) Magnesium maintains the length of the circadian period in
858 *Arabidopsis*. *Plant Physiol* **185**: 519–532
- 859 **Meng X, Wang Q, Hao R, Li X, Li M, Hu R, Du H, Hu Z, Yu B, Li S** (2022) RNA-binding
860 protein MAC5A interacts with the 26S proteasome to regulate DNA damage response in
861 *Arabidopsis*. *Plant Physiol* kiac510
- 862 **Monaghan J, Xu F, Gao M, Zhao Q, Palma K, Long C, Chen S, Zhang Y, Li X** (2009) Two
863 Prp19-like U-box proteins in the MOS4-associated complex play redundant roles in plant
864 innate immunity. *PLoS Pathog* **5**: e1000526
- 865 **Nohales MA, Kay SA** (2016) Molecular mechanisms at the core of the plant circadian oscillator.
866 *Nat Struct Mol Biol* **23**: 1061–1069
- 867 **Nolte C, Staiger D** (2015) RNA around the clock - regulation at the RNA level in biological
868 timing. *Front Plant Sci* **6**: 311
- 869 **Perez-Santángelo S, Mancini E, Francey LJ, Schlaen RG, Chernomoretz A, Hogenesch JB,**
870 **Yanovsky MJ** (2014) Role for LSM genes in the regulation of circadian rhythms. *Proc*
871 *Natl Acad Sci U S A* **111**: 15166–15171
- 872 **Plautz JD, Straume M, Stanewsky R, Jamison CF, Brandes C, Dowse HB, Hall JC, Kay SA**
873 (1997) Quantitative analysis of *Drosophila* period gene transcription in living animals. *J*
874 *Biol Rhythms* **12**: 204–217
- 875 **Romanowski A, Schlaen RG, Perez-Santangelo S, Mancini E, Yanovsky MJ** (2020) Global
876 transcriptome analysis reveals circadian control of splicing events in *Arabidopsis thaliana*.
877 *Plant J* **103**: 889–902

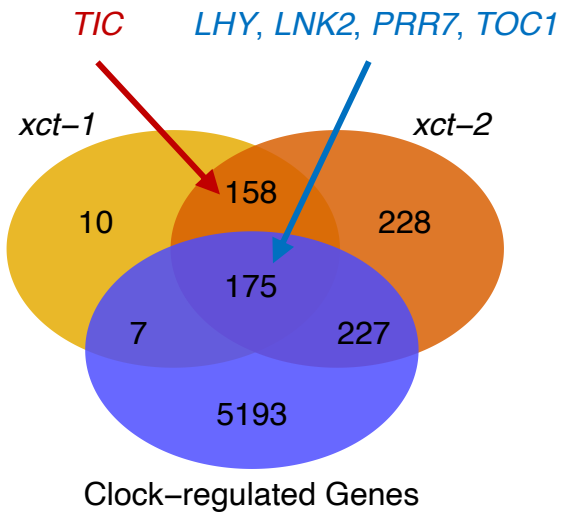
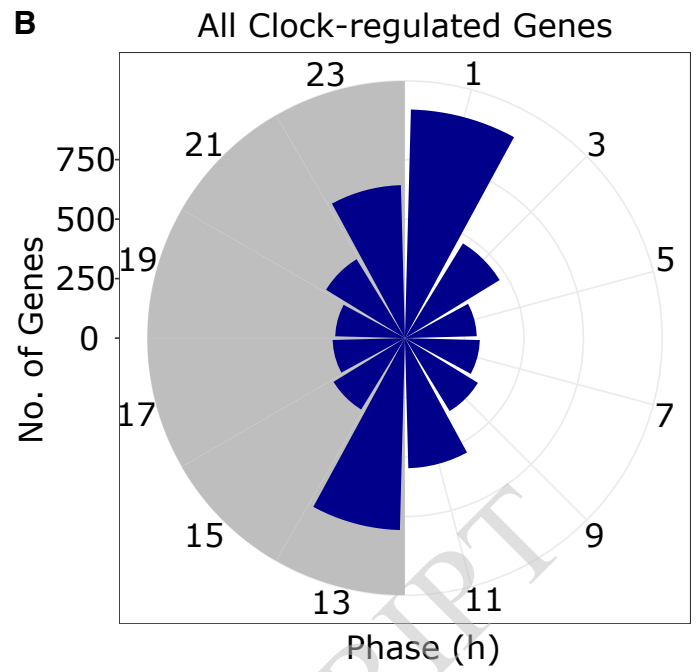
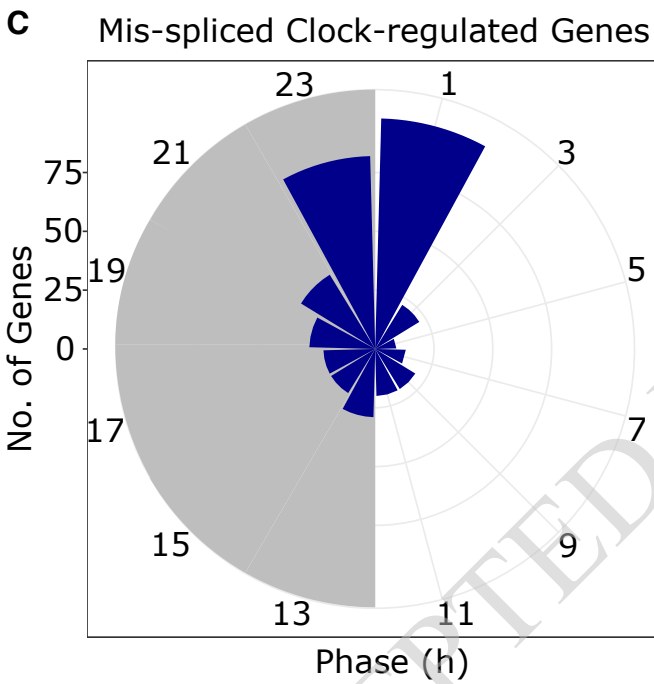
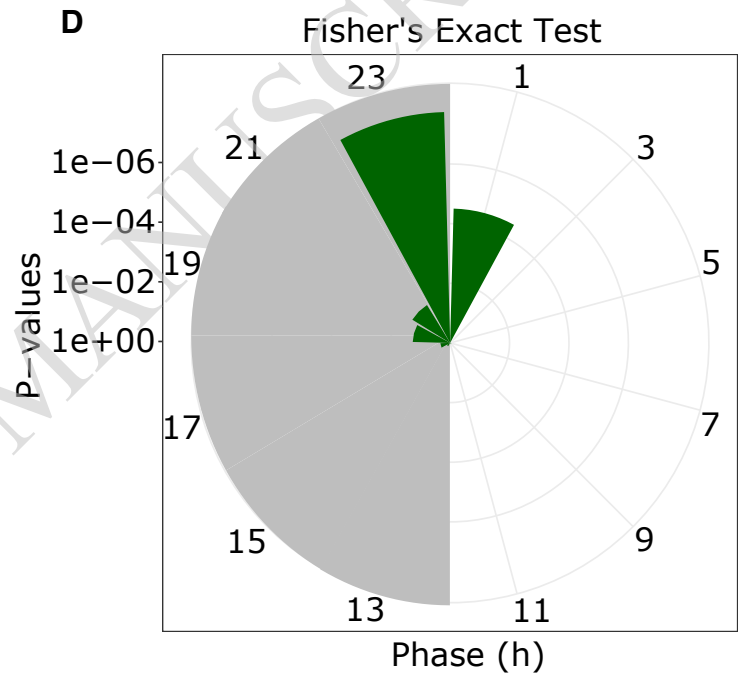
- 878 **Sanchez SE, Petrillo E, Beckwith EJ, Zhang X, Rugnone ML, Hernando CE, Cuevas JC,**
879 **Godoy Herz MA, Depetris-Chauvin A, Simpson CG, et al** (2010) A methyl transferase
880 links the circadian clock to the regulation of alternative splicing. *Nature* **468**: 112–116
- 881 **Schlaen RG, Mancini E, Sanchez SE, Perez-Santángelo S, Rugnone ML, Simpson CG,**
882 **Brown JWS, Zhang X, Chernomoretz A, Yanovsky MJ** (2015) The spliceosome
883 assembly factor GEMIN2 attenuates the effects of temperature on alternative splicing and
884 circadian rhythms. *Proc Natl Acad Sci U S A* **112**: 9382–9387
- 885 **Semlow DR, Blanco MR, Walter NG, Staley JP** (2016) Spliceosomal DEAH-Box ATPases
886 Remodel Pre-mRNA to Activate Alternative Splice Sites. *Cell* **164**: 985–998
- 887 **Seo PJ, Park M-J, Lim M-H, Kim S-G, Lee M, Baldwin IT, Park C-M** (2012) A self-
888 regulatory circuit of CIRCADIAN CLOCK-ASSOCIATED1 underlies the circadian
889 clock regulation of temperature responses in Arabidopsis. *Plant Cell* **24**: 2427–2442
- 890 **Shakhmantsir I, Sehgal A** (2019) Splicing the Clock to Maintain and Entrain Circadian
891 Rhythms. *J Biol Rhythms* **34**: 584–595
- 892 **Shi Y** (2017) Mechanistic insights into precursor messenger RNA splicing by the spliceosome.
893 *Nat Rev Mol Cell Biol* **18**: 655–670
- 894 **Uehara TN, Nonoyama T, Taki K, Kuwata K, Sato A, Fujimoto KJ, Hirota T, Matsuo H,**
895 **Maeda AE, Ono A, et al** (2022) Phosphorylation of RNA Polymerase II by CDKC2
896 Maintains the Arabidopsis Circadian Clock Period. *Plant Cell Physiol* **63**: 450–462
- 897 **Wang B-B, Brendel V** (2006) Genomewide comparative analysis of alternative splicing in
898 plants. *Proc Natl Acad Sci U S A* **103**: 7175–7180
- 899 **Wang X, Wu F, Xie Q, Wang H, Wang Y, Yue Y, Gahura O, Ma S, Liu L, Cao Y, et al**
900 (2012) SKIP is a component of the spliceosome linking alternative splicing and the
901 circadian clock in Arabidopsis. *Plant Cell* **24**: 3278–3295

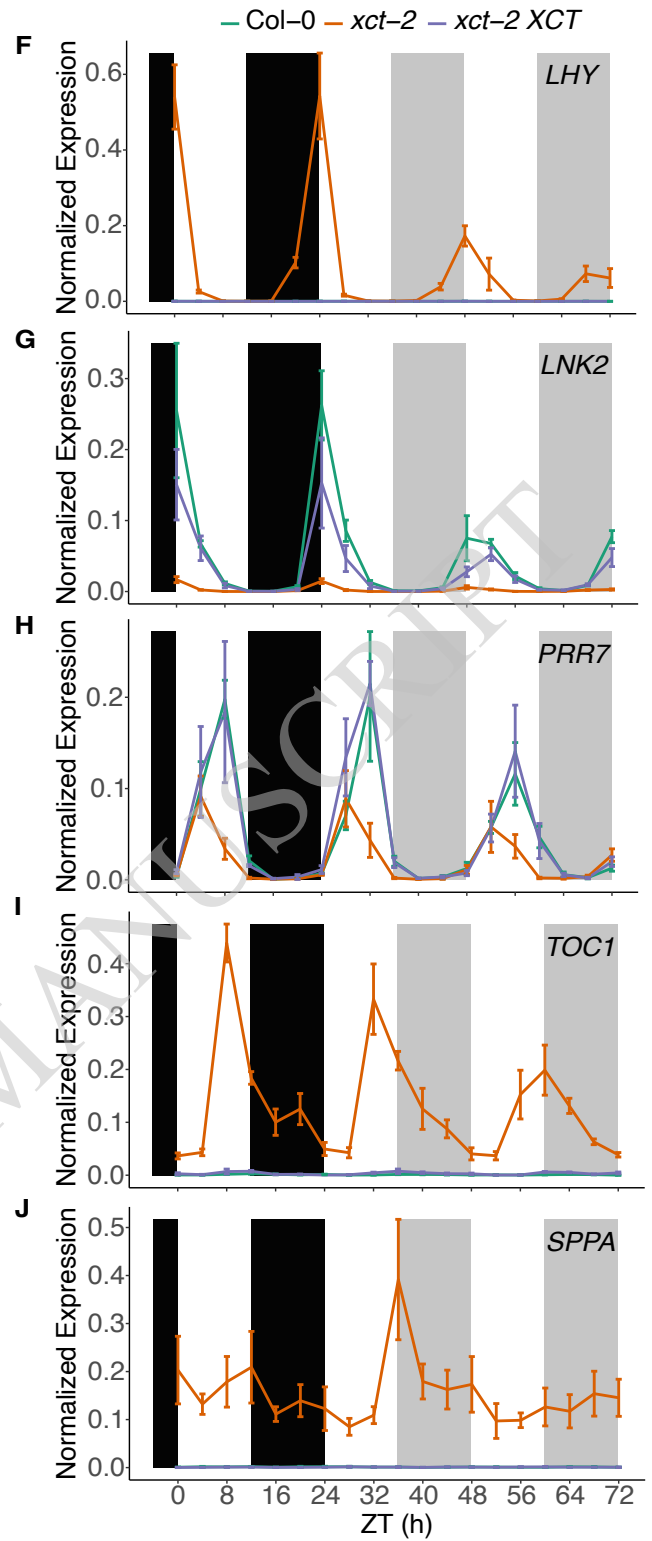
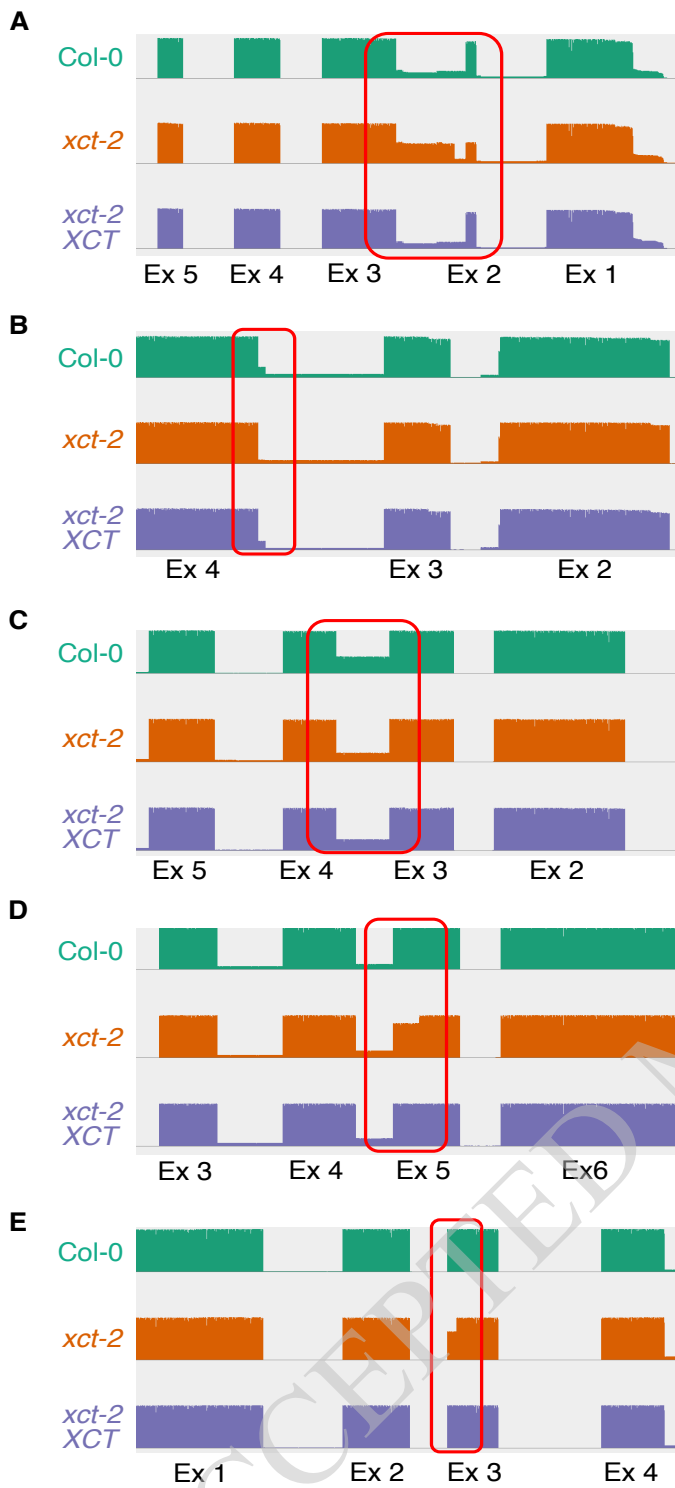
- 902 **Wei Y, Yee PP, Liu Z, Zhang L, Guo H, Zheng H, Anderson B, Gulley M, Li W (2020)**
903 **NEDD4L-mediated Merlin ubiquitination facilitates Hippo pathway activation. EMBO**
904 **Rep 21: e50642**
- 905 **Wilkinson ME, Charenton C, Nagai K (2020) RNA Splicing by the Spliceosome. Annu Rev**
906 **Biochem 89: 359–388**
- 907 **Xu Y-J, Lei Y, Li R, Zhang L-L, Zhao Z-X, Zhao J-H, Fan J, Li Y, Yang H, Shang J, et al**
908 **(2017) XAP5 CIRCADIAN TIMEKEEPER Positively Regulates RESISTANCE TO**
909 **POWDERY MILDEW8.1-Mediated Immunity in Arabidopsis. Front Plant Sci 8: 2044**
- 910 **Yang Y, Li Y, Sancar A, Oztas O (2020) The circadian clock shapes the Arabidopsis**
911 **transcriptome by regulating alternative splicing and alternative polyadenylation. J Biol**
912 **Chem 295: 7608–7619**
- 913 **Zhan X, Lu Y, Zhang X, Yan C, Shi Y (2022) Mechanism of exon ligation by human**
914 **spliceosome. Mol Cell 82: 2769-2778.e4**
- 915 **Zhang S, Liu Y, Yu B (2014) PRL1, an RNA-binding protein, positively regulates the**
916 **accumulation of miRNAs and siRNAs in Arabidopsis. PLoS Genet 10: e1004841**
- 917 **Zhang S, Xie M, Ren G, Yu B (2013) CDC5, a DNA binding protein, positively regulates**
918 **posttranscriptional processing and/or transcription of primary microRNA transcripts.**
919 **Proc Natl Acad Sci U S A 110: 17588–17593**

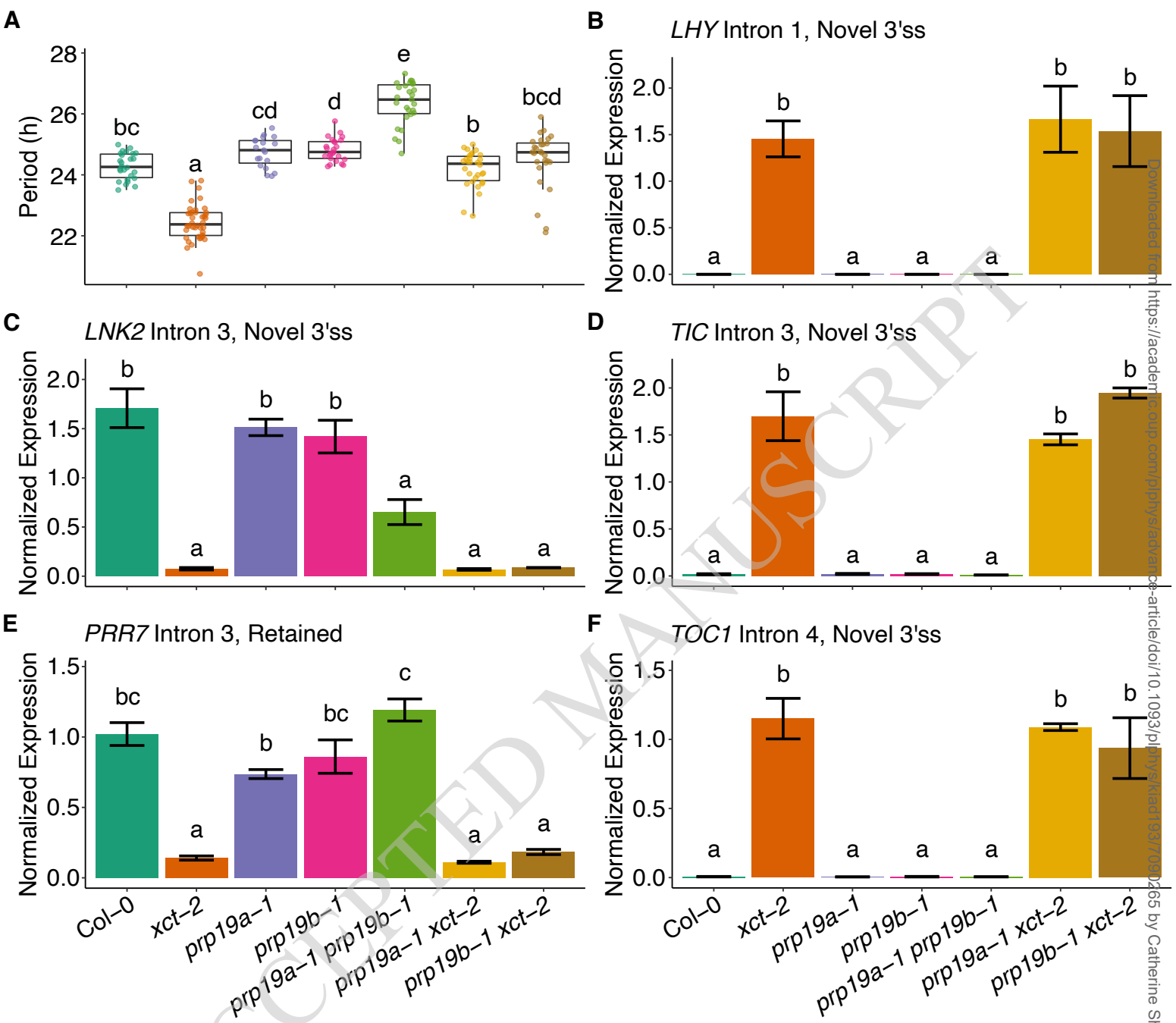






A**B****C****D**





Parsed Citations

Anver S, Roguev A, Zofall M, Krogan NJ, Grewal SIS, Harmer SL (2014) Yeast X-chromosome-associated protein 5 (Xap5) functions with H2AZ to suppress aberrant transcripts. *EMBO Rep* 15: 894–902

Google Scholar: [Author Only](#) [Title Only](#) [Author and Title](#)

Bessonov S, Anokhina M, Krasauskas A, Golas MM, Sander B, Will CL, Urlaub H, Stark H, Lührmann R (2010) Characterization of purified human Bact spliceosomal complexes reveals compositional and morphological changes during spliceosome activation and first step catalysis. *RNA* 16: 2384–2403

Google Scholar: [Author Only](#) [Title Only](#) [Author and Title](#)

Bessonov S, Anokhina M, Will CL, Urlaub H, Lührmann R (2008) Isolation of an active step I spliceosome and composition of its RNP core. *Nature* 452: 846–850

Google Scholar: [Author Only](#) [Title Only](#) [Author and Title](#)

Chanarat S, Seizl M, Strässer K (2011) The Prp19 complex is a novel transcription elongation factor required for TREX occupancy at transcribed genes. *Genes Dev* 25: 1147–1158

Google Scholar: [Author Only](#) [Title Only](#) [Author and Title](#)

Chanarat S, Strässer K (2013) Splicing and beyond: the many faces of the Prp19 complex. *Biochim Biophys Acta* 1833: 2126–2134

Google Scholar: [Author Only](#) [Title Only](#) [Author and Title](#)

Clough SJ, Bent AF (1998) Floral dip: a simplified method for *Agrobacterium*-mediated transformation of *Arabidopsis thaliana*. *Plant J* 16: 735–743

Google Scholar: [Author Only](#) [Title Only](#) [Author and Title](#)

Covington MF, Harmer SL (2007) The circadian clock regulates auxin signaling and responses in *Arabidopsis*. *PLoS Biol* 5: e222

Google Scholar: [Author Only](#) [Title Only](#) [Author and Title](#)

Creux N, Harmer S (2019) Circadian Rhythms in Plants. *Cold Spring Harb Perspect Biol* 11: a034611

Google Scholar: [Author Only](#) [Title Only](#) [Author and Title](#)

Deng X, Lu T, Wang L, Gu L, Sun J, Kong X, Liu C, Cao X (2016) Recruitment of the NineTeen Complex to the activated spliceosome requires AtPRMT5. *Proc Natl Acad Sci U S A* 113: 5447–5452

Google Scholar: [Author Only](#) [Title Only](#) [Author and Title](#)

Fang X, Shi Y, Lu X, Chen Z, Qi Y (2015) CMA33/XCT Regulates Small RNA Production through Modulating the Transcription of Dicer-Like Genes in *Arabidopsis*. *Mol Plant* 8: 1227–1236

Google Scholar: [Author Only](#) [Title Only](#) [Author and Title](#)

Feki A, Liu W, Hong J, Li M-W, Lee C-M, Zhou EK, Gendron JM (2019) Decoys provide a scalable platform for the identification of plant E3 ubiquitin ligases that regulate circadian function. *Elife* 8: e44558

Google Scholar: [Author Only](#) [Title Only](#) [Author and Title](#)

Filichkin SA, Priest HD, Givan SA, Shen R, Bryant DW, Fox SE, Wong W-K, Mockler TC (2010) Genome-wide mapping of alternative splicing in *Arabidopsis thaliana*. *Genome Res* 20: 45–58

Google Scholar: [Author Only](#) [Title Only](#) [Author and Title](#)

Harmer SL (2009) The circadian system in higher plants. *Annu Rev Plant Biol* 60: 357–377

Google Scholar: [Author Only](#) [Title Only](#) [Author and Title](#)

Hartley SW, Mullikin JC (2016) Detection and visualization of differential splicing in RNA-Seq data with JunctionSeq. *Nucleic Acids Res* 44: e127

Google Scholar: [Author Only](#) [Title Only](#) [Author and Title](#)

Hartley SW, Mullikin JC (2015) QoRTs: a comprehensive toolset for quality control and data processing of RNA-Seq experiments. *BMC Bioinformatics* 16: 224

Google Scholar: [Author Only](#) [Title Only](#) [Author and Title](#)

Hatakeyama S, Yada M, Matsumoto M, Ishida N, Nakayama KI (2001) U box proteins as a new family of ubiquitin-protein ligases. *J Biol Chem* 276: 33111–33120

Google Scholar: [Author Only](#) [Title Only](#) [Author and Title](#)

Hogg R, McGrail JC, O'Keefe RT (2010) The function of the NineTeen Complex (NTC) in regulating spliceosome conformations and fidelity during pre-mRNA splicing. *Biochem Soc Trans* 38: 1110–1115

Google Scholar: [Author Only](#) [Title Only](#) [Author and Title](#)

Horowitz DS (2012) The mechanism of the second step of pre-mRNA splicing. *Wiley Interdiscip Rev RNA* 3: 331–350

Google Scholar: [Author Only](#) [Title Only](#) [Author and Title](#)

- Hsu PY, Harmer SL (2012) Circadian phase has profound effects on differential expression analysis. *PLoS One* 7: e49853
Google Scholar: [Author Only](#) [Title Only](#) [Author and Title](#)
- Hsu PY, Harmer SL (2014) Wheels within wheels: the plant circadian system. *Trends Plant Sci* 19: 240–249
Google Scholar: [Author Only](#) [Title Only](#) [Author and Title](#)
- Idrissou M, Maréchal A (2022) The PRP19 Ubiquitin Ligase, Standing at the Cross-Roads of mRNA Processing and Genome Stability. *Cancers (Basel)* 14: 878
Google Scholar: [Author Only](#) [Title Only](#) [Author and Title](#)
- James AB, Syed NH, Bordage S, Marshall J, Nimmo GA, Jenkins GI, Herzyk P, Brown JWS, Nimmo HG (2012) Alternative splicing mediates responses of the Arabidopsis circadian clock to temperature changes. *Plant Cell* 24: 961–981
Google Scholar: [Author Only](#) [Title Only](#) [Author and Title](#)
- Jia T, Zhang B, You C, Zhang Y, Zeng L, Li S, Johnson KCM, Yu B, Li X, Chen X (2017) The Arabidopsis MOS4-Associated Complex Promotes MicroRNA Biogenesis and Precursor Messenger RNA Splicing. *Plant Cell* 29: 2626–2643
Google Scholar: [Author Only](#) [Title Only](#) [Author and Title](#)
- Jones MA, Williams BA, McNicol J, Simpson CG, Brown JWS, Harmer SL (2012) Mutation of Arabidopsis spliceosomal timekeeper locus1 causes circadian clock defects. *Plant Cell* 24: 4066–4082
Google Scholar: [Author Only](#) [Title Only](#) [Author and Title](#)
- Klaric JA, Wüst S, Panier S (2021) New Faces of old Friends: Emerging new Roles of RNA-Binding Proteins in the DNA Double-Strand Break Response. *Front Mol Biosci* 8: 668821
Google Scholar: [Author Only](#) [Title Only](#) [Author and Title](#)
- Koncz C, Dejong F, Villacorta N, Szakonyi D, Koncz Z (2012) The spliceosome-activating complex: molecular mechanisms underlying the function of a pleiotropic regulator. *Front Plant Sci* 3: 9
Google Scholar: [Author Only](#) [Title Only](#) [Author and Title](#)
- Kumimoto RW, Ellison CT, Toruño TY, Bak A, Zhang H, Casteel CL, Coaker G, Harmer SL (2021) XAP5 CIRCADIAN TIMEKEEPER Affects Both DNA Damage Responses and Immune Signaling in Arabidopsis. *Front Plant Sci* 12: 707923
Google Scholar: [Author Only](#) [Title Only](#) [Author and Title](#)
- Kwon Y-J, Park M-J, Kim S-G, Baldwin IT, Park C-M (2014) Alternative splicing and nonsense-mediated decay of circadian clock genes under environmental stress conditions in Arabidopsis. *BMC Plant Biol* 14: 136
Google Scholar: [Author Only](#) [Title Only](#) [Author and Title](#)
- Lee Y-R, Khan K, Armfield-Uhas K, Srikanth S, Thompson NA, Pardo M, Yu L, Norris JW, Peng Y, Gripp KW, et al (2020) Mutations in FAM50A suggest that Armfield XLID syndrome is a spliceosomopathy. *Nat Commun* 11: 3698
Google Scholar: [Author Only](#) [Title Only](#) [Author and Title](#)
- Li L, Tian G, Peng H, Meng D, Wang L, Hu X, Tian C, He M, Zhou J, Chen L, et al (2018) New class of transcription factors controls flagellar assembly by recruiting RNA polymerase II in Chlamydomonas. *Proc Natl Acad Sci U S A* 115: 4435–4440
Google Scholar: [Author Only](#) [Title Only](#) [Author and Title](#)
- Li Y, Yang J, Shang X, Lv W, Xia C, Wang C, Feng J, Cao Y, He H, Li L, et al (2019) SKIP regulates environmental fitness and floral transition by forming two distinct complexes in Arabidopsis. *New Phytol* 224: 321–335
Google Scholar: [Author Only](#) [Title Only](#) [Author and Title](#)
- Liu L, Li X, Yuan L, Zhang G, Gao H, Xu X, Zhao H (2022) XAP5 CIRCADIAN TIMEKEEPER specifically modulates 3' splice site recognition and is important for circadian clock regulation partly by alternative splicing of LHY and TIC. *Plant Physiol Biochem* 172: 151–157
Google Scholar: [Author Only](#) [Title Only](#) [Author and Title](#)
- Maréchal A, Li J-M, Ji XY, Wu C-S, Yazinski SA, Nguyen HD, Liu S, Jiménez AE, Jin J, Zou L (2014) PRP19 transforms into a sensor of RPA-ssDNA after DNA damage and drives ATR activation via a ubiquitin-mediated circuitry. *Mol Cell* 53: 235–246
Google Scholar: [Author Only](#) [Title Only](#) [Author and Title](#)
- Marshall CM, Tartaglio V, Duarte M, Harmon FG (2016) The Arabidopsis sickle Mutant Exhibits Altered Circadian Clock Responses to Cool Temperatures and Temperature-Dependent Alternative Splicing. *Plant Cell* 28: 2560–2575
Google Scholar: [Author Only](#) [Title Only](#) [Author and Title](#)
- Martin-Tryon EL, Harmer SL (2008) XAP5 CIRCADIAN TIMEKEEPER coordinates light signals for proper timing of photomorphogenesis and the circadian clock in Arabidopsis. *Plant Cell* 20: 1244–1259
Google Scholar: [Author Only](#) [Title Only](#) [Author and Title](#)
- Martin-Tryon EL, Kreps JA, Harmer SL (2007) GIGANTEA acts in blue light signaling and has biochemically separable roles in circadian clock and flowering time regulation. *Plant Physiol* 143: 473–486
Google Scholar: [Author Only](#) [Title Only](#) [Author and Title](#)

Mayas RM, Maita H, Staley JP (2006) Exon ligation is proofread by the DEXD/H-box ATPase Prp22p. *Nat Struct Mol Biol* 13: 482–490

Google Scholar: [Author Only](#) [Title Only](#) [Author and Title](#)

de Melo JRF, Gutsch A, Caluwé TD, Leloup J-C, Gonze D, Hermans C, Webb AAR, Verbruggen N (2021) Magnesium maintains the length of the circadian period in *Arabidopsis*. *Plant Physiol* 185: 519–532

Google Scholar: [Author Only](#) [Title Only](#) [Author and Title](#)

Meng X, Wang Q, Hao R, Li X, Li M, Hu R, Du H, Hu Z, Yu B, Li S (2022) RNA-binding protein MAC5A interacts with the 26S proteasome to regulate DNA damage response in *Arabidopsis*. *Plant Physiol* 191: 510–520

Google Scholar: [Author Only](#) [Title Only](#) [Author and Title](#)

Monaghan J, Xu F, Gao M, Zhao Q, Palma K, Long C, Chen S, Zhang Y, Li X (2009) Two Prp19-like U-box proteins in the MOS4-associated complex play redundant roles in plant innate immunity. *PLoS Pathog* 5: e1000526

Google Scholar: [Author Only](#) [Title Only](#) [Author and Title](#)

Nohales MA, Kay SA (2016) Molecular mechanisms at the core of the plant circadian oscillator. *Nat Struct Mol Biol* 23: 1061–1069

Google Scholar: [Author Only](#) [Title Only](#) [Author and Title](#)

Nolte C, Staiger D (2015) RNA around the clock - regulation at the RNA level in biological timing. *Front Plant Sci* 6: 311

Google Scholar: [Author Only](#) [Title Only](#) [Author and Title](#)

Perez-Santángelo S, Mancini E, Francey LJ, Schlaen RG, Chernomoretz A, Hogenesch JB, Yanovsky MJ (2014) Role for LSM genes in the regulation of circadian rhythms. *Proc Natl Acad Sci U S A* 111: 15166–15171

Google Scholar: [Author Only](#) [Title Only](#) [Author and Title](#)

Plautz JD, Straume M, Stanewsky R, Jamison CF, Brandes C, Dowse HB, Hall JC, Kay SA (1997) Quantitative analysis of *Drosophila* period gene transcription in living animals. *J Biol Rhythms* 12: 204–217

Google Scholar: [Author Only](#) [Title Only](#) [Author and Title](#)

Romanowski A, Schlaen RG, Perez-Santángelo S, Mancini E, Yanovsky MJ (2020) Global transcriptome analysis reveals circadian control of splicing events in *Arabidopsis thaliana*. *Plant J* 103: 889–902

Google Scholar: [Author Only](#) [Title Only](#) [Author and Title](#)

Sanchez SE, Petrillo E, Beckwith EJ, Zhang X, Rugnone ML, Hernando CE, Cuevas JC, Godoy Herz MA, Depetris-Chauvin A, Simpson CG, et al (2010) A methyl transferase links the circadian clock to the regulation of alternative splicing. *Nature* 468: 112–116

Google Scholar: [Author Only](#) [Title Only](#) [Author and Title](#)

Schlaen RG, Mancini E, Sanchez SE, Perez-Santángelo S, Rugnone ML, Simpson CG, Brown JWS, Zhang X, Chernomoretz A, Yanovsky MJ (2015) The spliceosome assembly factor GEMIN2 attenuates the effects of temperature on alternative splicing and circadian rhythms. *Proc Natl Acad Sci U S A* 112: 9382–9387

Google Scholar: [Author Only](#) [Title Only](#) [Author and Title](#)

Semlow DR, Blanco MR, Walter NG, Staley JP (2016) Spliceosomal DEAH-Box ATPases Remodel Pre-mRNA to Activate Alternative Splice Sites. *Cell* 164: 985–998

Google Scholar: [Author Only](#) [Title Only](#) [Author and Title](#)

Seo PJ, Park M-J, Lim M-H, Kim S-G, Lee M, Baldwin IT, Park C-M (2012) A self-regulatory circuit of CIRCADIAN CLOCK-ASSOCIATED1 underlies the circadian clock regulation of temperature responses in *Arabidopsis*. *Plant Cell* 24: 2427–2442

Google Scholar: [Author Only](#) [Title Only](#) [Author and Title](#)

Shakhmantsir I, Sehgal A (2019) Splicing the Clock to Maintain and Entrain Circadian Rhythms. *J Biol Rhythms* 34: 584–595

Google Scholar: [Author Only](#) [Title Only](#) [Author and Title](#)

Shi Y (2017) Mechanistic insights into precursor messenger RNA splicing by the spliceosome. *Nat Rev Mol Cell Biol* 18: 655–670

Google Scholar: [Author Only](#) [Title Only](#) [Author and Title](#)

Uehara TN, Nonoyama T, Taki K, Kuwata K, Sato A, Fujimoto KJ, Hirota T, Matsuo H, Maeda AE, Ono A, et al (2022) Phosphorylation of RNA Polymerase II by CDKC2 Maintains the *Arabidopsis* Circadian Clock Period. *Plant Cell Physiol* 63: 450–462

Google Scholar: [Author Only](#) [Title Only](#) [Author and Title](#)

Wang B-B, Brendel V (2006) Genomewide comparative analysis of alternative splicing in plants. *Proc Natl Acad Sci U S A* 103: 7175–7180

Google Scholar: [Author Only](#) [Title Only](#) [Author and Title](#)

Wang X, Wu F, Xie Q, Wang H, Wang Y, Yue Y, Gahura O, Ma S, Liu L, Cao Y, et al (2012) SKIP is a component of the spliceosome linking alternative splicing and the circadian clock in *Arabidopsis*. *Plant Cell* 24: 3278–3295

Google Scholar: [Author Only](#) [Title Only](#) [Author and Title](#)

Wei Y, Yee PP, Liu Z, Zhang L, Guo H, Zheng H, Anderson B, Gulley M, Li W (2020) NEDD4L-mediated Merlin ubiquitination facilitates Hippo pathway activation. *EMBO Rep* 21: e50642

Google Scholar: [Author Only](#) [Title Only](#) [Author and Title](#)

Wilkinson ME, Charenton C, Nagai K (2020) RNA Splicing by the Spliceosome. *Annu Rev Biochem* 89: 359–388

Google Scholar: [Author Only](#) [Title Only](#) [Author and Title](#)

Xu Y-J, Lei Y, Li R, Zhang L-L, Zhao Z-X, Zhao J-H, Fan J, Li Y, Yang H, Shang J, et al (2017) XAP5 CIRCADIAN TIMEKEEPER Positively Regulates RESISTANCE TO POWDERY MILDEW8.1-Mediated Immunity in Arabidopsis. *Front Plant Sci* 8: 2044

Google Scholar: [Author Only](#) [Title Only](#) [Author and Title](#)

Yang Y, Li Y, Sancar A, Oztas O (2020) The circadian clock shapes the Arabidopsis transcriptome by regulating alternative splicing and alternative polyadenylation. *J Biol Chem* 295: 7608–7619

Google Scholar: [Author Only](#) [Title Only](#) [Author and Title](#)

Zhan X, Lu Y, Zhang X, Yan C, Shi Y (2022) Mechanism of exon ligation by human spliceosome. *Mol Cell* 82: 2769-2778.e4

Google Scholar: [Author Only](#) [Title Only](#) [Author and Title](#)

Zhang S, Liu Y, Yu B (2014) PRL1, an RNA-binding protein, positively regulates the accumulation of miRNAs and siRNAs in Arabidopsis. *PLoS Genet* 10: e1004841

Google Scholar: [Author Only](#) [Title Only](#) [Author and Title](#)

Zhang S, Xie M, Ren G, Yu B (2013) CDC5, a DNA binding protein, positively regulates posttranscriptional processing and/or transcription of primary microRNA transcripts. *Proc Natl Acad Sci U S A* 110: 17588–17593

Google Scholar: [Author Only](#) [Title Only](#) [Author and Title](#)

ACCEPTED MANUSCRIPT